Hierarchies of stratigraphic discontinuity surfaces in siliciclastic, carbonate and mixed siliciclastic-bioclastic tidalites

Implications for fluid migration in reservoir quality assessment

Chiarella, Domenico; Longhitano, Sergio G.; Spalluto, Luigi; Martinius, Allard W.

DOI
10.1002/dep2.307

Publication date
2024

Document Version
Final published version

Published in
Depositional Record

Citation (APA)
Chiarella, D., Longhitano, S. G., Spalluto, L., & Martinius, A. W. (2024). Hierarchies of stratigraphic discontinuity surfaces in siliciclastic, carbonate and mixed siliciclastic-bioclastic tidalites: Implications for fluid migration in reservoir quality assessment. *Depositional Record*, *11*(1), 373-402. https://doi.org/10.1002/dep2.307

Received: 30 November 2023 | Revised: 16 July 2024 | Accepted: 29 July 2024

DOI: 10.1002/dep2.307

The Depositional Record
A journal of the International Association of Sedimentologists
Open Access
IAS
WILEY

ORIGINAL ARTICLE

Hierarchies of stratigraphic discontinuity surfaces in siliciclastic, carbonate and mixed siliciclastic-bioclastic tidalites: Implications for fluid migration in reservoir quality assessment

Domenico Chiarella[1] | **Sergio G. Longhitano**[2] | **Luigi Spalluto**[3] | **Allard W. Martinius**[4,5]

[1]Department of Earth Sciences, Royal Holloway, University of London, Egham, UK

[2]Department of Sciences, University of Basilicata, Potenza, Italy

[3]Department of Earth and Geoenvironmental Sciences, University of Bari, Bari, Italy

[4]Equinor Research Centre, Trondheim, Norway

[5]Faculty of Civil Engineering and Geosciences, Delft University of Technology, Delft, The Netherlands

Correspondence
Domenico Chiarella, Department of Earth Sciences, Royal Holloway, University of London, Egham, UK.
Email: domenico.chiarella@rhul.ac.uk

Funding information
Università degli Studi della Basilicata, Grant/Award Number: 432/2012

Abstract

The hierarchies of the stratigraphic discontinuity surfaces observed in ancient tidalites are qualitatively assessed, aiming to evaluate their role as possible preferential conduits for fluid migration. Three outcrop examples are presented from microtidal settings of southern Italy: (i) siliciclastic tidalites consisting of quartz-rich cross-stratified sandstones generated by strong two-directional tidal currents flowing along a tidal strait; (ii) carbonate tidalites, which accumulated in a Cretaceous lagoon and tidal flat where peritidal cycles formed vertically-stacked sequences of biopeloidal and fenestral packstones, wackestones and bindstones during repeated phases of Milankovitch-scale sea-level changes; (iii) mixed, siliciclastic-bioclastic tidalites, deposited in a bay and recording offshore-transition, to shoreface wave-dominated and tide-influenced environments. Observations made during this study suggest that fluid movement can be controlled by the presence of main bounding surfaces that occur at different dimensions, from large (hectometre)-scale, to medium (decametre)-scale, to smaller (metre)-scales. These surfaces produced either by depositional or erosional processes, are characterised by different features and geometries in siliciclastic, carbonate and mixed siliciclastic-bioclastic tidalites arguably revealing complex internal pathways for fluid flows. These results suggest that fluids propagating along the main discontinuities follow a dominant sub-horizontal direction of propagation, associated with minor sub-vertical movements, due to local internal surface geometries and interconnections and a general lack of fractures. This surface-based approach to the study of fluid-flow transmission within stratified rocks represents a conceptual attempt to predict fluid mobility and reservoir potential in tidalite-bearing siliciclastic, carbonate and mixed reservoir rocks.

KEYWORDS
bioclastic, carbonate, fluid migration, reservoir, siliciclastic, stratigraphic surfaces, tidalites

1 | INTRODUCTION

The current energy transition and net zero scenario have led to increased interest in understanding reservoir properties at different observational scales. In this context, fluid migration and permanent sequestration in the subsurface is becoming an important mechanism in carbon neutralisation (Ringrose & Meckel, 2019; Payton et al., 2021, 2022a; Jackson et al., 2022). Sedimentary successions formed in tidal dominated/influenced environments represent reservoir plays of worldwide economic importance for the energy transition because they are in many instances well-suited for CO_2 storage (Ambrose et al., 2008; Aker et al., 2011, 2021; Sundal et al., 2014, 2016; Benson et al., 2018; Furre et al., 2019; Jackson et al., 2022; Meneguolo et al., 2022; Hossain et al., 2024). The characterisation of tide-influenced to tide-dominated facies and assessment of reservoir quality is often challenging and strongly controlled by their multiscale heterogenic architecture and property distribution (Wen et al., 1998; Jackson et al., 1999, 2022; Martinius et al., 2001, 2005; Nordahl et al., 2005; Ringrose et al., 2005). Fluid flow in reservoirs is affected by heterogeneity at a range of scales, from large (hectometre)-scale to micro (micron)-scale with the main control exerted by bedding surfaces, facies and grain textural changes (Weber, 1986; Weber & van Geuns, 1990; Pickup et al., 1994; Pickup & Hern, 2002; Grammer et al., 2004; Payton et al., 2022a, 2022b). Accordingly, the characterisation of bounding and internal either erosional or depositional discontinuity surfaces plays a key role. However, in spite of the profusion of publications on clastic tidally-generated sediments there are few reservoir quality studies which approach the analysis of tidalites from the perspective of their bounding and internal discontinuity surfaces (Wen et al., 1998; Nordahl et al., 2005; Ringrose et al., 2005; Araújo et al., 2021; Khan et al., 2023).

Sediments involved in tidal processes are mainly transported and repeatedly reworked by alternating flood and ebb-driven currents, so that 'tidalites' (i.e. sedimentary accumulations produced by tidally-driven depositional processes, sensu Williams, 1991 and Kvale, 2003) commonly result in highly-heterogeneous deposits, characterised by specific facies assemblages, including tidal rhythmites, bundle cross lamination, flaser, wavy and lenticular bedding, herringbone structures, etc. (see review in Coughenour et al., 2009; Dalrymple, 2010; Longhitano et al., 2012).

Surfaces and their lithological contrasts, bounding sedimentary bedforms at laminae-scale to compound dune-scale or bar-scale and parasequence-scale, control to a large extent fluid flow through reservoirs formed by these deposits and provide crucial information necessary to characterise in a qualitative and quantitative sense. This data can subsequently be deployed to build heterogeneity-scale surface-based specific models and used for fluid-flow analysis with or without adding property trends for each lithofacies (Agar & Geiger, 2015).

In general, surface-based facies characterisation and modelling studies (Jackson et al., 2013) at different scales of sedimentary heterogeneity has focussed on deep-marine (Pyrczs et al., 2005; Zhang et al., 2009), shoreface (Sech et al., 2009) and marginal marine tide-influenced or tide-dominated systems (White & Barton, 1999; White et al., 2004; Elfenbein et al., 2005; Jackson et al., 2005, 2009; Nordahl et al., 2005; Massart et al., 2012, 2016; Jacquemyn et al., 2021). Moreover, a number of studies have investigated in particular the effect of bounding surfaces at small scale (laminae to facies association) for CO_2 migration in aeolian (Newell et al., 2019), fluvial (Alshakri et al., 2023; Issautier et al., 2013; Olierook et al., 2014; Sun et al., 2023; Trevisan, 2017a, 2017b), shallow marine (Mishra et al., 2020) and carbonate (Casteleyn et al., 2010; Chandra et al., 2015; Araújo et al., 2021; Pourmalek et al., 2021a; Li et al., 2022) environments.

Pourmalek et al. (2021b) described the facies interplay and associated sediment heterogeneity of three variations of mixed carbonate-siliciclastic reservoirs. They showed that storage security increased when these reservoir types had a strong layering developed at facies association level (the large-scale bounding surface class discussed below). Storage capacity was found to be controlled by: (i) heterogeneity, (ii) permeability of each facies (i.e. permeability contrast; see also Casteleyn et al. (2010) for carbonate facies related property distributions and their effect on CO_2 storage) and (iii) the degree of heterogeneity (e.g. the Late Permian Grayburg Formation; Casteleyn et al., 2010). Only a few studies on surface-based facies characterisation and rock typing of carbonate or mixed siliciclastic-carbonate sandstone deposits (excluding constructive carbonate deposits such as platforms, reefs, etc.), for the purpose of studying flow behaviour, are available.

The present study aims to provide new information on discrete bounding surface heterogeneities resulting from sediment transport (erosion and deposition) and associated conceptual models that can be used in fluid flow modelling. Three well-documented field examples are reviewed to conceptually describe surface-based depositional models that can facilitate fluid flow analysis in siliciclastic, carbonate and mixed siliciclastic-bioclastic tidalites. The three case studies derive from two middle-upper Pliocene and a lower Pleistocene succession exposed in southern Italy and interpreted as the record of an ancient tidal strait (i.e. the Catanzaro Strait), a palaeo-bay (i.e. Acerenza Bay), and a Cretaceous tidal flat of the Apulia Carbonate Platform, respectively. These field-based examples are compared to evaluate in two-dimensions the role of their stratigraphic discontinuity surfaces in a reservoir characterisation framework. These surfaces occur at multiple length scales in tidal deposits.

2 | GEOLOGICAL SETTING OF THE THREE STUDIED AREAS

The tidal deposits examined in the present study are located in three different sectors of southern Italy: the Lucanian Apennine, which is a segment of the wider southern Apennine, the Apulia Carbonate Platform and the Calabrian Arc (Figure 1). The Lucanian Apennine is an east-verging fold-and-thrust belt (Figure 1), built on the western border of the Apulia Carbonate Platform from late Oligocene–early Miocene times (Pescatore et al., 1999). From the Miocene onwards, the thrust front migrated progressively eastwards, and during the Pliocene and Pleistocene, several wedge-top marine basins developed within the tectonic accretionary prism (Vezzani, 1967; Hippolyte et al., 1994; Pieri et al., 1994). In some of these basins, coastal embayments favoured a tidal influence on the sublittoral sedimentation (Longhitano, 2011; Chiarella & Longhitano, 2012; Longhitano et al., 2012b). The areas around the village of Acerenza preserves a number of outcrops, the best exposed of which has been analysed in this study.

The Apulia Carbonate Platform (Figure 1) represents the foreland of the southern Apennine Chain (Selli, 1962; Ricchetti et al., 1988; D'Argenio et al., 2004) (Figure 1). Its sedimentary succession cropping out in the Murge area, consists of 3000 m thick Cretaceous limestones and dolostones deposited mainly in shallow-water environments (Ciaranfi et al., 1988; Spalluto et al., 2005, 2007, 2008; Spalluto, 2008, 2012). This succession includes one major regional intra-Cretaceous unconformity produced by a long-lasting episode of subaerial exposure during the Turonian (Valduga, 1965; Ricchetti, 1975; Mindszenty et al., 1995). Below this unconformity, parallel-bedded, mud-supported limestones with frequent intercalations of dolostones, containing poorly differentiated microfossiliferous assemblages, recorded tidal flat environments (Spalluto, 2012).

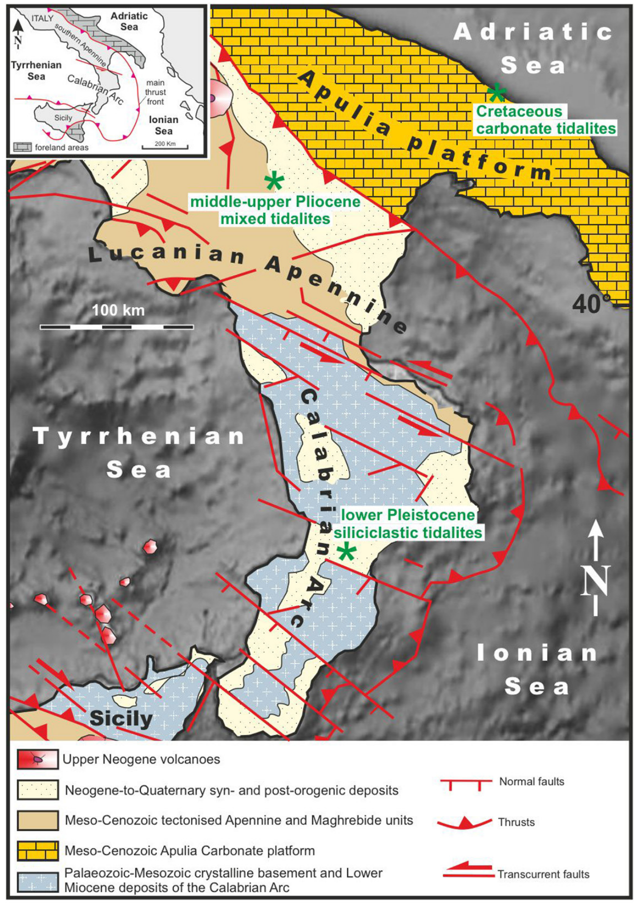

FIGURE 1 Geotectonic map of southern Italy (inset), showing the main areas where tidalites (asterisks) were documented: The Lucanian Apennine and the Calabrian Arc (modified from Longhitano et al., 2012b).

The Calabrian Arc mainly consists of late Palaeozoic metamorphic and intrusive rocks, tectonically superposed on ophiolite-bearing units of Tethyan affinity, in turn overlying Mesozoic carbonate platform limestone of Apennine affinity (Tortorici, 1982). The Neogene to Quaternary tectonic evolution of the Calabrian Arc led to the formation of a series of half-grabens and narrow-linear basins, some of these acting as tidal straits, including the Amantea, the Catanzaro, the Siderno and the Messina straits (Mercier et al., 1987; Colella, 1995; Longhitano & Nemec, 2005; Di Stefano & Longhitano, 2009; Longhitano et al., 2012, 2014; Longhitano, 2013; Chiarella et al., 2021) (Figure 1). The Catanzaro Strait is used as an example for the outcrop analysed in this study.

3 | GENERAL SEDIMENTOLOGICAL FEATURES OF THE TIDAL DEPOSITS

3.1 | Siliciclastic tidalites of the Catanzaro palaeo-strait

The lower Pleistocene (Calabrian) deposits in the Catanzaro Basin (Figure 2A) consist of large-scale cross-strata-sets (Figure 3), ranging in thickness from 10 to 15 m along the basin margins, up to 35 m across the basin centre, accumulated in a tectonically-confined strait during a rapid phase of transgression (Chiarella, 2011, 2016; Longhitano, 2011, 2013; Chiarella et al., 2012a; Longhitano et al., 2012d, 2014; Longhitano & Chiarella, 2020). This sandy succession overlies Middle-Upper (?) Pliocene claystone/sandstone deposits over an unconformity, which grades into a conformity within the deepest parts of the basin. Laterally and vertically, the tidally-dominated sandy deposits grade into highly bioturbated fine-grained sandstone and siltstones (Figure 3) with a total thickness of 60 m.

The studied succession includes both two-dimensional (2D) and three-dimensional (3D) cross-strata dominated by siliciclastic material and supplemented by a subordinate amount of bioclasts (Chiarella, 2011; Chiarella et al., 2012a; Longhitano et al., 2014). The deposits are characterised by extensive erosional surfaces bounding the main cross-strata sets, the latter ranging from 1 up to 6 m in thickness (Figure 2B). Beds form simple and compound tidal cross-strata, interpreted as the building blocks of larger tidal dunes. Internally, cross-strata include tidal bundles of neap/spring and semi-diurnal duration (Longhitano, 2011; Longhitano et al., 2014; Longhitano & Chiarella, 2020).

3.1.1 | Facies heterogeneities and main bounding surfaces

Four main facies have been detected in this succession having complex lateral and vertical relationships. (i) Basal gravel/shell lags occur as erosionally-based, discontinuous layers of scattered or clustered polymictic gravels with clasts up to 0.5 m in diameter, passing laterally into densely packed shell beds, 0.5–1 m thick. The deposit consists of abundant articulated organisms in both life position and as shell lags, including skeletal assemblages of mollusc associations (up to 10% of the total volume) mixed up with gravel-size polymictic clasts. (ii) The overlying cross-strata sets form a sandbody up to 15 m thick, whose original lenticular or dune shape is locally still recognisable (Figure 4A). It includes vertically-stacked 2D and 3D smaller cross-strata, up to 1.5 m thick. (iii) The 3D cross-strata consist of moderately sorted coarse to very-coarse sand with dispersed granules and small pebbles, organised into concave-based lenticular bedsets 1 to 7 m thick. The main bounding surfaces have generally concave-up geometries (Figure 4B,C). Internally, foresets show both angular and tangential geometries with NNW-SSE palaeocurrents (Chiarella, 2011, 2016; Chiarella et al., 2012a; Longhitano et al., 2014; Chiarella & Gioia, 2021). Foreset laminae display grain-size contrasts of granule-size and sand-size clasts. The bioclastic content (*ca* 25%) consists of bryozoans, echinoids, molluscs and a variable percentage of foraminifera. Upwards, these sediments evolve to (iv) 2D cross-strata composed of medium to coarse-grained sand with rare granules and less abundant bioclasts (*ca* 10%). Strata have a tabular geometry with bed thickness ranging from 1 up to 6 m (Figure 4D). Internally, cross-strata show simple and compound architecture (cf. Dalrymple, 1984; Dalrymple & Rhodes, 1995). Local discontinuity surfaces bound smaller, ripple-scale strata which, in turn, are characterised by internal third-order discontinuity surfaces, interpreted as pause (or reactivation) planes (Figure 4E). The 3D and 2D tidal cross-strata pass laterally and upwards to (v) bioturbated sandstone and siltstone. This facies consists of very-fine to fine sand organised into thinly-bedded rippled strata, alternating with faintly-laminated siltstone strata. Primary structures are difficult to detect because of the very intense homogenisation exerted by a pervasive bioturbation. Upwards, this facies shows a monotonous, intensively bioturbated succession.

3.1.2 | Depositional processes and environments

Sedimentary facies recognised in the Catanzaro strait-fill succession record a tide-dominated subaqueous setting of a narrow passageway linking two adjacent

FIGURE 2 (A) Geological sketch of the Catanzaro area (modified from Chiarella, 2011) and (B) general stratigraphy of its Miocene-to-Quaternary sedimentary infill, including siliciclastic tidalite-bearing sandstones. (C) Geological map of the Apulian Carbonate Platform (modified from Spalluto, 2012) and (D) stratigraphic column of the Albian-Cenomanian succession (Calcare di Bari Fm) containing the carbonate tidalites described in this study. (E) Geological map of the Acerenza palaeobay in the Southern Apennine (modified, from Chiarella et al., 2012b) and (F) general basin stratigraphy showing the mixed tidalites studied in the present work.

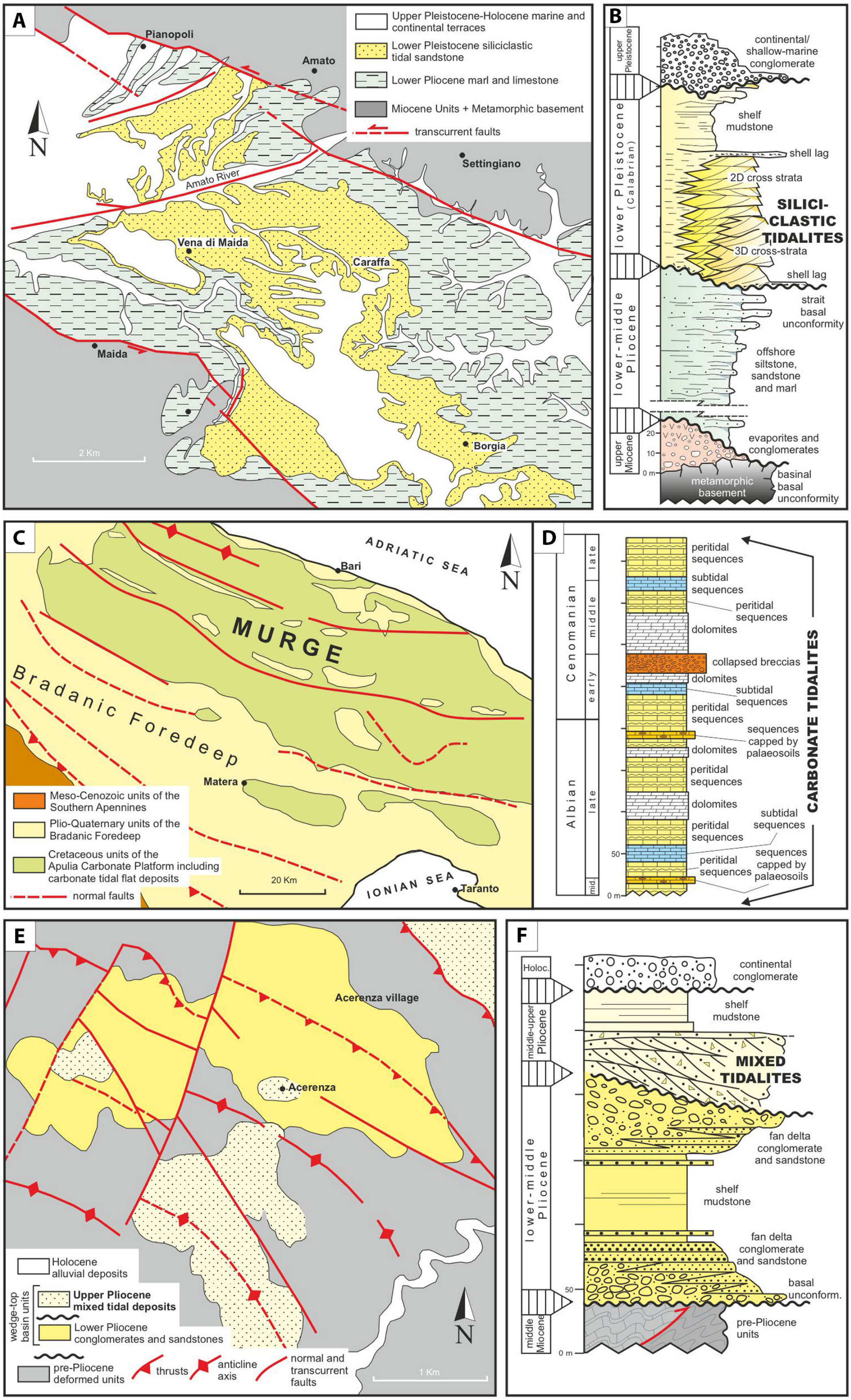
A
Pianopoli
Amato
Settingiano
Amato River
Vena di Maida
Caraffa
Maida
Borgia
2 Km
N
Upper Pleistocene-Holocene marine and continental terraces
Lower Pleistocene siliciclastic tidal sandstone
Lower Pliocene marl and limestone
Miocene Units + Metamorphic basement
transcurrent faults
B
upper Pleistocene
lower Pleistocene (Calabrian)
lower-middle Pliocene
upper Miocene
continental/ shallow-marine conglomerate
shelf mudstone
shell lag
2D cross strata
SILICI-CLASTIC TIDALITES
3D cross-strata
shell lag
strait basal unconformity
offshore siltstone, sandstone and marl
evaporites and conglomerates
metamorphic basement
basinal basal unconformity
20
10
0 m
C
ADRIATIC SEA
Bari
MURGE
Bradanic Foredeep
Matera
IONIAN SEA
Taranto
20 Km
N
Meso-Cenozoic units of the Southern Apennines
Plio-Quaternary units of the Bradanic Foredeep
Cretaceous units of the Apulia Carbonate Platform including carbonate tidal flat deposits
normal faults
D
Cenomanian
late
middle
early
Albian
late
mid.
peritidal sequences
subtidal sequences
peritidal sequences
dolomites
collapsed breccias
dolomites
subtidal sequences
peritidal sequences
sequences capped by palaeosoils
dolomites
peritidal sequences
dolomites
subtidal sequences
peritidal sequences
peritidal sequences
sequences capped by palaeosoils
CARBONATE TIDALITES
50
0 m
E
Acerenza village
Acerenza
1 Km
N
Holocene alluvial deposits
wedge-top basin units
Upper Pliocene mixed tidal deposits
Lower Pliocene conglomerates and sandstones
pre-Pliocene deformed units
thrusts
anticline axis
normal and transcurrent faults
F
Holoc.
middle-upper Pliocene
lower-middle Pliocene
middle Miocene
continental conglomerate
shelf mudstone
MIXED TIDALITES
fan delta conglomerate and sandstone
shelf mudstone
fan delta conglomerate and sandstone
basal unconform.
pre-Pliocene units
50
0 m

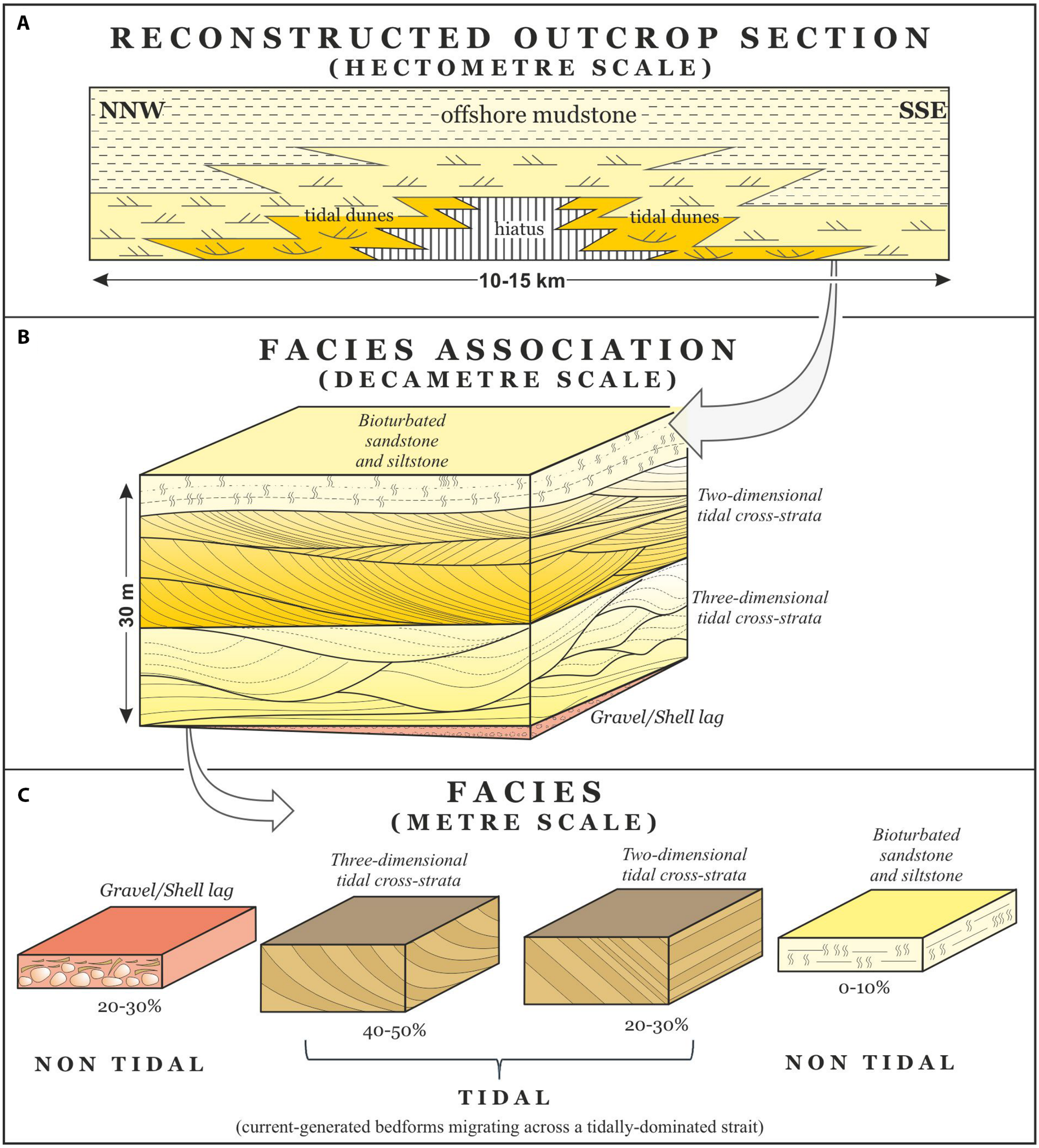

FIGURE 3 Hierarchies of sediment bodies and associated bounding surfaces in the lower Pleistocene Catanzaro strait-fill siliciclastic succession. (A) Basin-scale model (note the transgressive vertical trend). (B) Outcrop-scale facies association of the siliciclastic tidal cross-strata filling the strait, showing the vertical transition from 3D to 2D tidal bedforms, and to offshore mudstone. (C) Main tidal and non-tidal facies recognised in the studied succession with the percentage of relative occurrence.

basins. Virtually continuous exchanges of marine waters between the two interconnected seas resulted in strong currents, flowing in two opposite directions and producing sediment transport and accumulation in different sectors of the strait. Gravel/shell lags are interpreted to be the result of an initial stage of high rates of bed-shear stress, exerted by currents flowing at their maximum velocity. As a result, energetic tidal flows are here capable of accumulating coarse-grained deposits, transporting in suspension (and/or saltation)

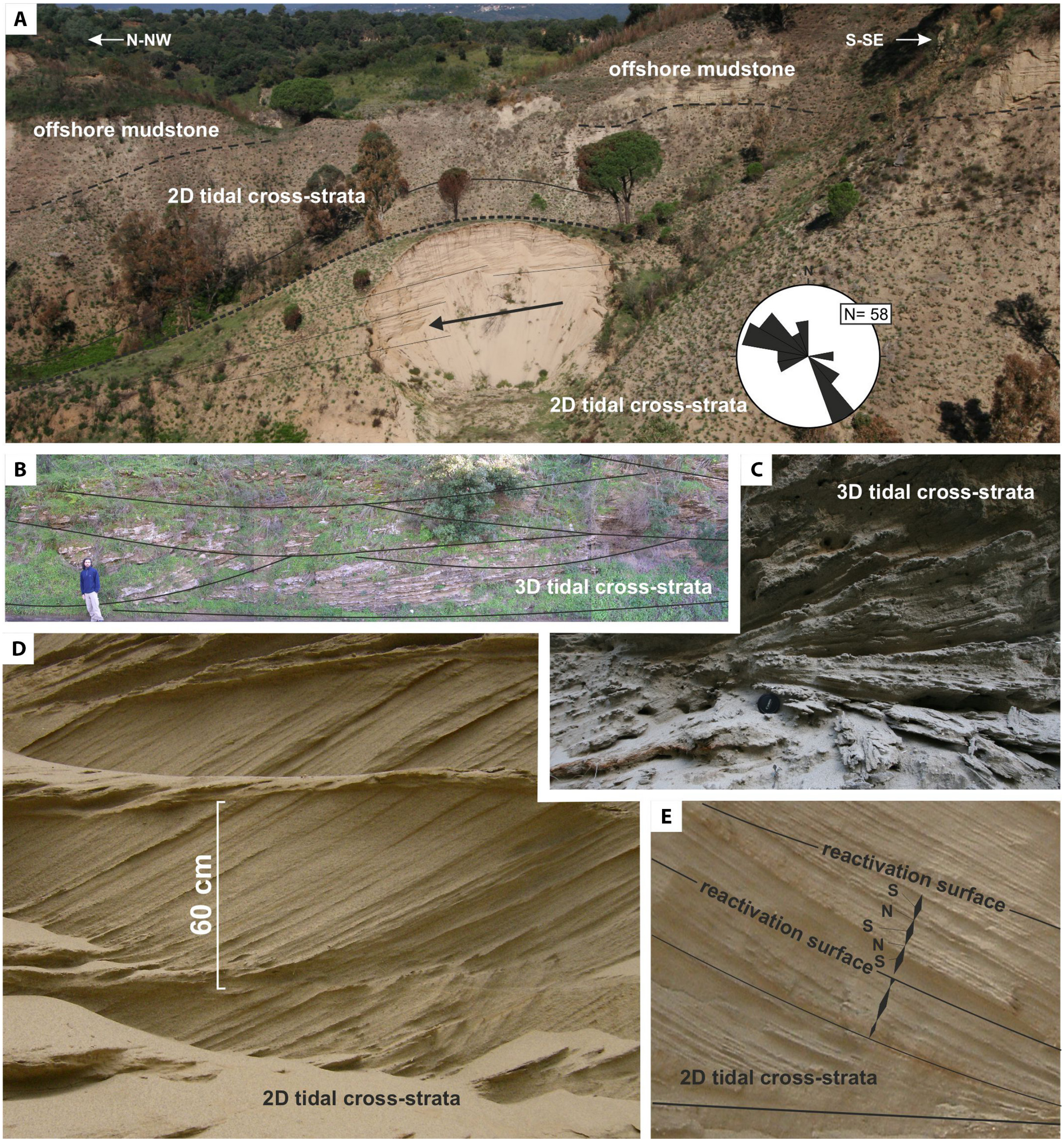

FIGURE 4 Outcrop exposure of the lower Pleistocene siliciclastic tidalites in the Catanzaro Strait. (A) Large-scale tidal compound cross-strata overlain by offshore mudstone. The bedform is about 18 m thick and is internally composed of forward-stacked, westward-migrating (arrow) 2D cross-strata. Palaeocurrents are 2D at basinal scale. (B) 3D tidal cross-strata and (C) detail of their internal heterogeneity (note the main discontinuity surfaces of erosional and depositional nature). (D) Vertically-stacked, 2D tidal cross-strata migrating toward the left of the photograph. (E) Detail from the previous outcrop showing internal reactivation surfaces and neap/spring (*N*/*S*) tidal cycles.

sand and mud-size sediments (Longhitano & Chiarella, 2020). This stage is known to characterise straits in their narrowest depositional zone (the ‘strait-centre zone’, cf. Longhitano, 2013). The overlying lithofacies indicates a significant change in the strait hydrodynamics, possibly due to a phase of relative sea-level rise (Chiarella, 2011; Longhitano et al., 2012d, 2014; Longhitano 2013; Longhitano & Chiarella, 2020). At the beginning of the transgression, 3D tidal dunes migrated throughout the *ca* 3–4 km wide and *ca* 30 km long, WNW-ESE-oriented

Catanzaro Strait, due to the continuous tidal circulation amplified through the basin and flowing in semi-diurnal phase opposition. As the intermediate phase of relative sea-level rise enlarged the strait width, the tidal current strength decreased because it was flowing in a wider cross-sectional area. The progressive reduction of the bed shear stress modified 3D tidal dunes into an extensive 2D bedform field. At the end of the transgression, the further widening of the Catanzaro Strait into an approximately 10–12 km wide marine passageway changed the tidally-dominated strait into a non-tidal open shelf (Chiarella et al., 2012a; Longhitano et al., 2014).

3.2 | Carbonate tidalites of the Apulia Platform

The Albian (*p.p.*)-upper Cenomanian stratigraphic succession of the Apulia Carbonate Platform (Figure 2C) is composed of an over 400 m thick sequence of shallow-water carbonates in the northern Murge area (Spalluto, 2012; Figure 2D). This succession mostly consists of vertically-stacked, tabular beds (Figure 5) as a result of the continued aggradation of shallow-water limestones in a subsiding area located along a mature passive margin (Ricchetti et al., 1988).

Despite its relatively simple architecture and monotonous facies tract, the vertical succession of these facies changed through time, showing a predominantly cyclic pattern of depositional and diagenetic features, both at bed and bedset scales (Spalluto et al., 2008; Spalluto, 2012). The occurrence of such sequences (comparable to 4th or 5th-order parasequences or simple sequences sensu Vail et al., 1991) is a very common and repetitive feature of shallow-water carbonates formed in peritidal environments (see Strasser et al., 1999).

3.2.1 | Facies heterogeneities and main bounding surfaces

The most abundant facies association recognised within the Cretaceous carbonate peritidal succession consists of mud-supported microfossiliferous limestones forming 'layer-cake' tabular beds whose general thickness ranges from a few decimetres to about 1.5 m. Four main facies have been described in this succession. At the bed scale, facies stack in peritidal cycles showing, from bottom to top, the following features (Figure 5B,C): (i) a few millimetres to a few centimetres thick basal intraclast-bearing deposits; (ii) *ca* 30–50 cm thick miliolid-ostracod-algal wackestones/packstones, consisting of intensely burrowed biopeloidal limestones showing a reduced diversity in benthonic organisms but commonly with a high number of individuals; (iii) *ca* 5–30 cm thick pelleted lime mudstones and wackestones, including sparse, small, thin-shelled ostracods, miliolids and gastropods, highly homogenised by burrowing; (iv) *ca* 5–30 cm thick fenestral wackestones/packstones (Figure 6A) or stromatolitic bindstones (Figure 6B) with peloids, micritic intraclasts, grapestones, mollusc fragments, small miliolids, tufts of porostromate cyanobacteria, *Thaumatoporella* sp. and ostracods. Internally, millimetre to centimetre-sized fenestral cavities (birdseyes) occur, forming laminoid or irregularly distributed spheroidal spar-filled voids which are often associated with microbial bindstones. Larger openings also occur, forming a dense network of irregularly shaped voids (stromatactoid fabric) locally filled with fine-grained geopetal sediments. The upper part of this facies also shows diffused mud cracks and/or a dense network of root traces (Figure 6C).

The above-described peritidal cycle represents the smallest recognisable facies sequence, or elementary sequence (sensu Strasser et al., 1999), capped by a discontinuity surface that frequently corresponds to a bed surface. The lateral continuity of such discontinuity surfaces is from several tens of metres to few hundreds of metres. The occurrence of fenestral limestones, microbial bindstones and root traces marks the discontinuity surface in the field.

At the bedset scale, elementary sequences are bundled in small-scale and medium-scale sequences (sensu Strasser et al., 1999). Small-scale sequences are composed of three to five elementary sequences, whereas medium-scale sequences are composed of three to four small-scale sequences (Spalluto, 2012). These sequences are bounded by discontinuity surfaces having a lateral continuity from several hundreds of metres to a few kilometres and, usually, exceed the lateral continuity of the outcrops. The occurrence of mud cracks and intraclastic flat-pebble intraclasts, large-sized dissolution fenestrae and pervasive burrowing by root traces mark these discontinuity surfaces in the field.

Locally, several elementary sequences are completely brecciated and form closely-spaced condensed stratigraphic intervals several kilometres in lateral extent. These intervals are bounded by the most relevant and laterally continuous discontinuity surfaces (Figure 6D). Intraclastic breccias are arranged in dense, grain-supported assemblages and form layers in which two parts with a different degree of cementation can be distinguished (Figure 6E). The lower part is chalky and intraclasts are embedded in a greenish or light brown silty-clayey matrix forming sheet-like horizons. Intraclast reworking is absent. This grades downwards into the underlying rock through a transition zone, showing strong evidence of in-situ alteration and brecciation. The upper part consists of intraclasts dominated

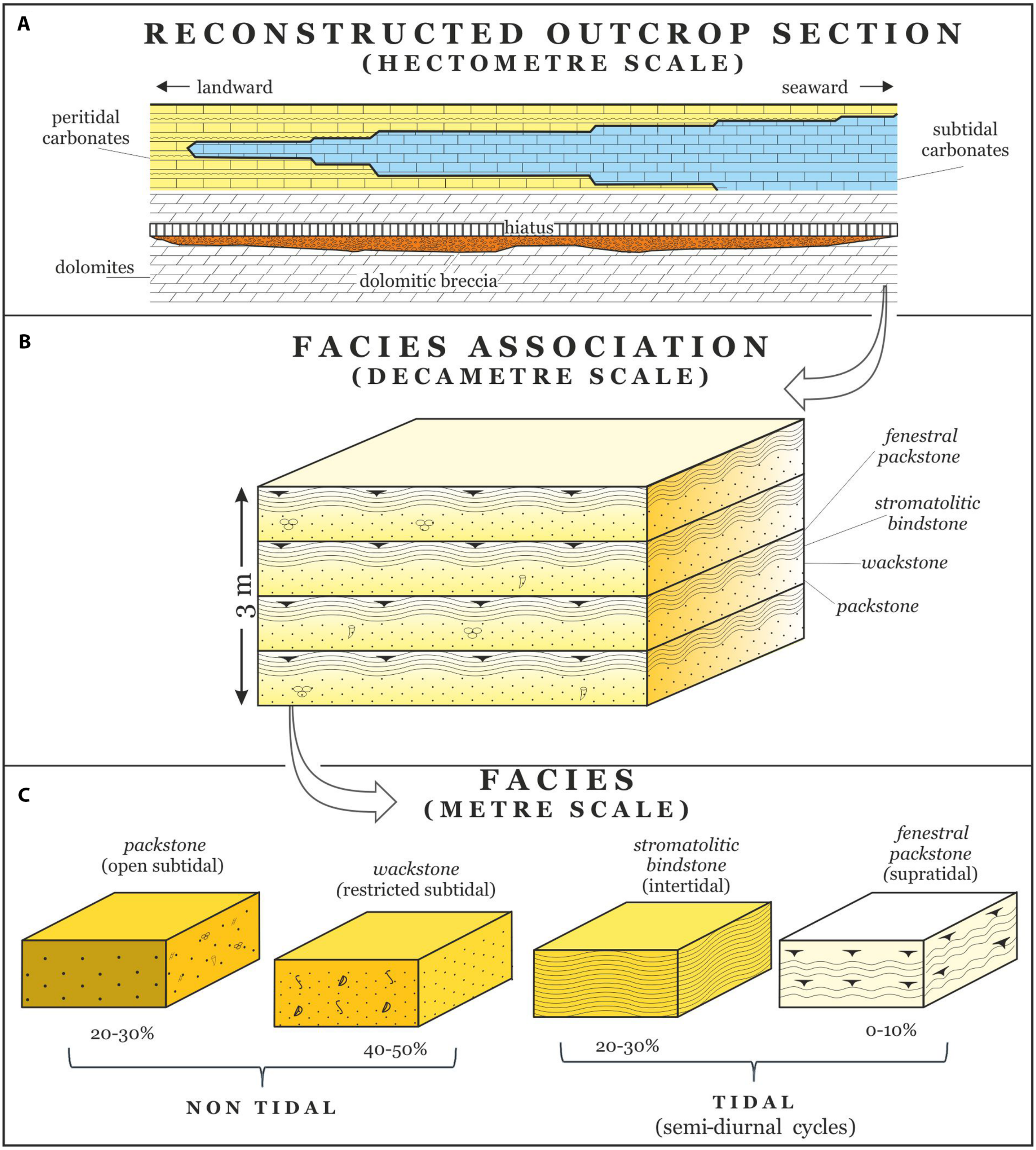

FIGURE 5 Hierarchies of sediment bodies in the Cretaceous Apulian Platform carbonate tidalites. (A) Basin-scale model (after Spalluto, 2012). (B) Outcrop-scale facies association of the carbonate deposits accumulated on a tidal flat. (C) Main facies recognised in the studied succession and relative occurrence expressed in percentages.

by black pebbles which are locally grouped into dark layers that are mostly concentrated at the top of this well-cemented interval. The matrix is commonly made up of clotted peloidal microcrystalline calcite. Root casts filled by dark micrite, cylindrical to irregular pores filled by sparite and circum-granular cracks also occur.

3.2.2 | Depositional processes and environments

Facies interpretation obtained from the studied succession suggests that basal intraclast-bearing deposits represent early transgressive reworked lags. The overlying

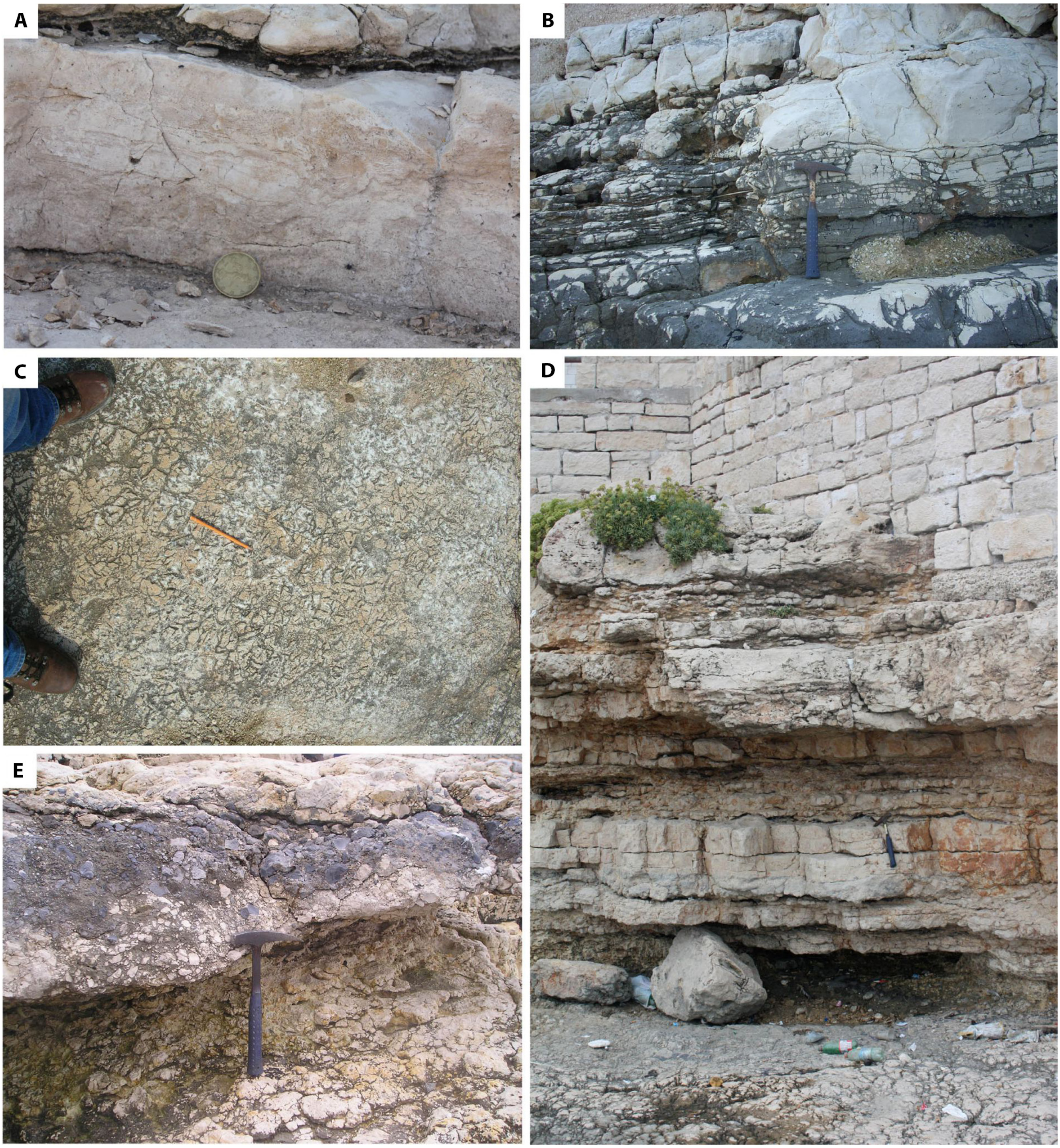

FIGURE 6 Outcrop exposure of the Cretaceous carbonate peritidal deposits in the Murge area. (A) Detail of the top of small-scale peritidal sequence. (B) Intertidal stromatolitic limestones showing the occurrence of desiccation features (mudcracks) in the upper part. (C) Detail of the upper part of a peritidal small-scale sequence showing a dense network of root traces developed in upper intertidal/lower supratidal environment. (D) Outcrop-scale peritidal cycles bounded by brecciated palaeosols. (E) Detail of the top of brecciated palaeosols showing grain-supported breccia layers, including black pebbles in the upper part.

association of miliolid-ostracod-algal wackestones/packstones, pelleted lime mudstones/wackestones and fenestral wackestones/packstones record the vertical stacking of subtidal, lower intertidal and upper intertidal/lower supratidal environments respectively. The presence of black pebbles confirms this interpretation since they are considered as important markers for partial or complete subaerial exposure (Strasser & Davaud, 1983; Flügel, 2004) and frequently occur in supratidal carbonates (Esteban & Klappa, 1983).

According to Shinn (1983), low-energy and semi-restricted shallow coastal area experienced the influence of semi-diurnal tidal cycles, which were responsible for short-lived exposure surfaces and the accompanying desiccation and incipient pedogenesis of the underlying carbonate tidalites. However, in this setting the tides alone are too small to have a significant effect on sediment deposition (Pratt, 2010). Therefore, tidal-influenced structures in peritidal carbonates have only been described at lamina-scale in microbial intertidal deposits (e.g. the millimetre-thick laminae of stromatolites) where they contribute to the trapping and binding of carbonate grains (Suarez-Gonzalez et al., 2014).

Peritidal carbonates reveal a hierarchical organisation in depositional sequences that is a recurrent feature described for several ancient carbonate platforms developed in greenhouse worlds (Strasser, 2018). Elementary, small-scale and medium-scale sequences found in the studied section are bounded by well-developed discontinuity surfaces. These surfaces form when vertical abrupt facies change and/or diagenetic contrast occur (Clari et al., 1995) and record short-lived interruption of carbonate sedimentation with hiatuses below biostratigraphic resolution (Hillgärtner, 1998). These latter features mostly form in supratidal environments even if some sequences may develop completely in fully subtidal conditions (Spalluto, 2012). Elementary sequences showing supratidal exposure often lack intertidal facies. In this case, typical features indicating supratidal exposure (e.g. root traces, brecciation and desiccation polygons) directly lie above restricted, mud-supported, shallow-subtidal deposits. The lack of intertidal facies often observed in peritidal sequences is attributed to subaerial exposure during the sea-level fall episodes, incomplete filling of the available accommodation space or deep pedogenetic alteration into the overlying palaeosols (Strasser, 1991).

Several lines of evidence seem to suggest that the peritidal Cretaceous carbonates of Southern Italy had a hierarchical organisation controlled by Earth's orbital forcing in the Milankovitch frequency band (D'Argenio et al., 2008). As a result, discontinuity surfaces in such carbonates have a clear hierarchical organisation and reflect different durations of subaerial exposure. Moreover, the development of major discontinuity surfaces at the top of a several metres thick condensed brecciated interval indicates that Milankovitch cycles are superimposed on long-term sea-level fluctuations. Consequently, during long-term sea-level falls the peritidal area underwent a significant loss of accommodation that allowed the development of laterally continuous palaeosols. These discontinuity surfaces thus indicate major sedimentary gaps in carbonate deposition corresponding to 3rd order sequence boundary (Strasser et al., 2000; Spalluto, 2012).

3.3 | Mixed siliciclastic-bioclastic tidalites of the southern Apennine

The siliciclastic/bioclastic deposits of Acerenza (Figure 2E) represent the shallow-water bay-fill of a peripheral coastal area of a Middle-Upper Pliocene wedge-top basin (Chiarella, 2011; Chiarella et al., 2012b, 2019; Longhitano et al., 2021). Sediments consist of a compositional mixing (sensu Chiarella et al., 2017) of siliciclastic and bioclastic components. Several types of cross-stratification indicate that different hydrodynamic conditions acted simultaneously in such a sublittoral setting, including waves and tidal currents (Chiarella, 2011; Chiarella et al., 2012b; Chiarella & Longhitano, 2012). Mixed sediments form a *ca* 30 m thick succession (Figure 2F), composed of three vertically-stacked stratal units. Individual stratal units are 5–15 m thick, show a shallowing-upward vertical facies succession and are separated by surfaces of marine flooding or by angular unconformities that become conformable surfaces basinwards. The studied succession includes both 2D and 3D tidal cross-strata, exhibiting a mixture of siliciclastic and carbonate grains (Chiarella, 2011; Chiarella et al., 2012b). Internally, mixed sediments frequently reveal bundles of well-segregated siliciclastic and bioclastic lamina-sets, diagnostic of mixed environments experiencing tidal influence (Longhitano, 2011; Chiarella & Longhitano, 2012; James et al., 2014).

3.3.1 | Facies heterogeneities and main bounding surfaces

Stratal units documented in the Acerenza section consist of a suite of several facies associations showing distinct degrees of heterolithic segregation between siliciclastic and bioclastic particles (Chiarella et al., 2012b; Chiarella & Longhitano, 2012). Each stratal unit (Figures 7A and 8A) is characterised by a basal sharp surface, overlain by lags of gravel and densely packed skeletal assemblages of bivalve, bryozoan and echinoid remains, forming 20–60 cm thick lenticular beds (Figures 7B and 8A). These deposits are overlain by a 1 m thick bioturbated coarse-grained interval, containing large *Thalassinoides*, *Conichnus*, *Piscichnus*, *Skolithos* and decimetre-scale, J-shaped burrows. This basal deposit passes upwards into three, vertically-stacked facies associations (Figure 8A). (i) The lowermost facies association includes 2D cross-strata of well-segregated particles (Figure 8B,C) and consists of medium-grained to coarse-grained, well-rounded siliciclastic-bioclastic sand, organised into planar cross-strata sets up to 1 m thick. Cross-strata (2D dunes) are stacked into co-sets bounded by planar, locally erosional, surfaces. Discontinuity surfaces are generally horizontal

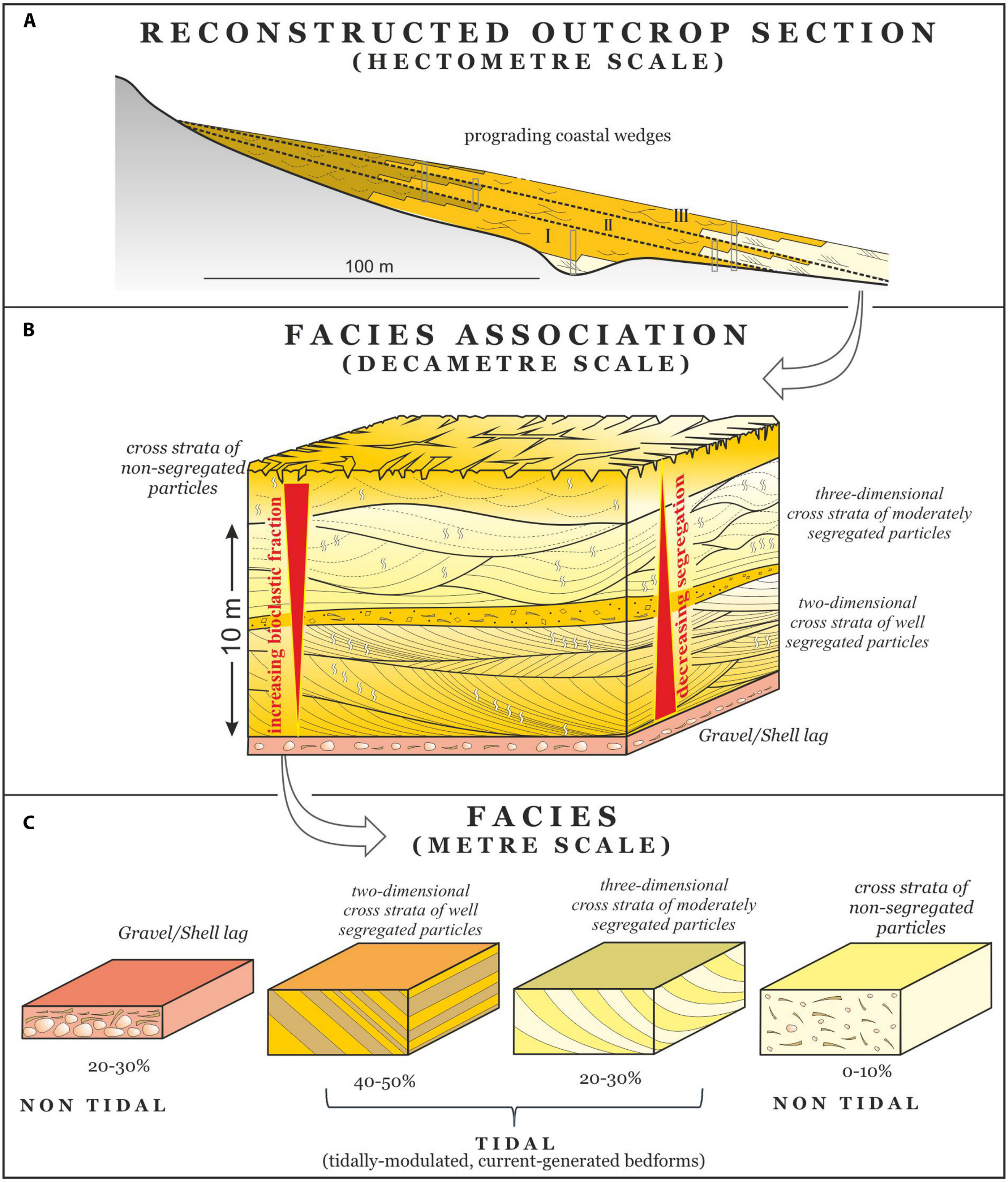

FIGURE 7 Hierarchies of sediment bodies in the lower-middle Pliocene Acerenza bay-fill mixed succession. (A) Reconstructed geological profile including the three stratal units (I, II and III) and recording a prograding coastal wedge (note the regressive vertical trend of each unit) (from Chiarella & Longhitano, 2012). (B) Outcrop-scale facies association of the tide-influenced mixed deposits showing the vertical transition from 2D to 3D dunes. (C) Main facies recognised in the studied succession and relative percentages.

and characterise bases and tops of single beds. Strata consist of repeated bundles of well-segregated siliciclastic/thicker and bioclastic/thinner lamina-sets (Chiarella & Longhitano, 2012; Figure 8C). Foresets show angular and tangential basal contacts with a slightly concave frontal profile. They are mainly unidirectional, although foresets

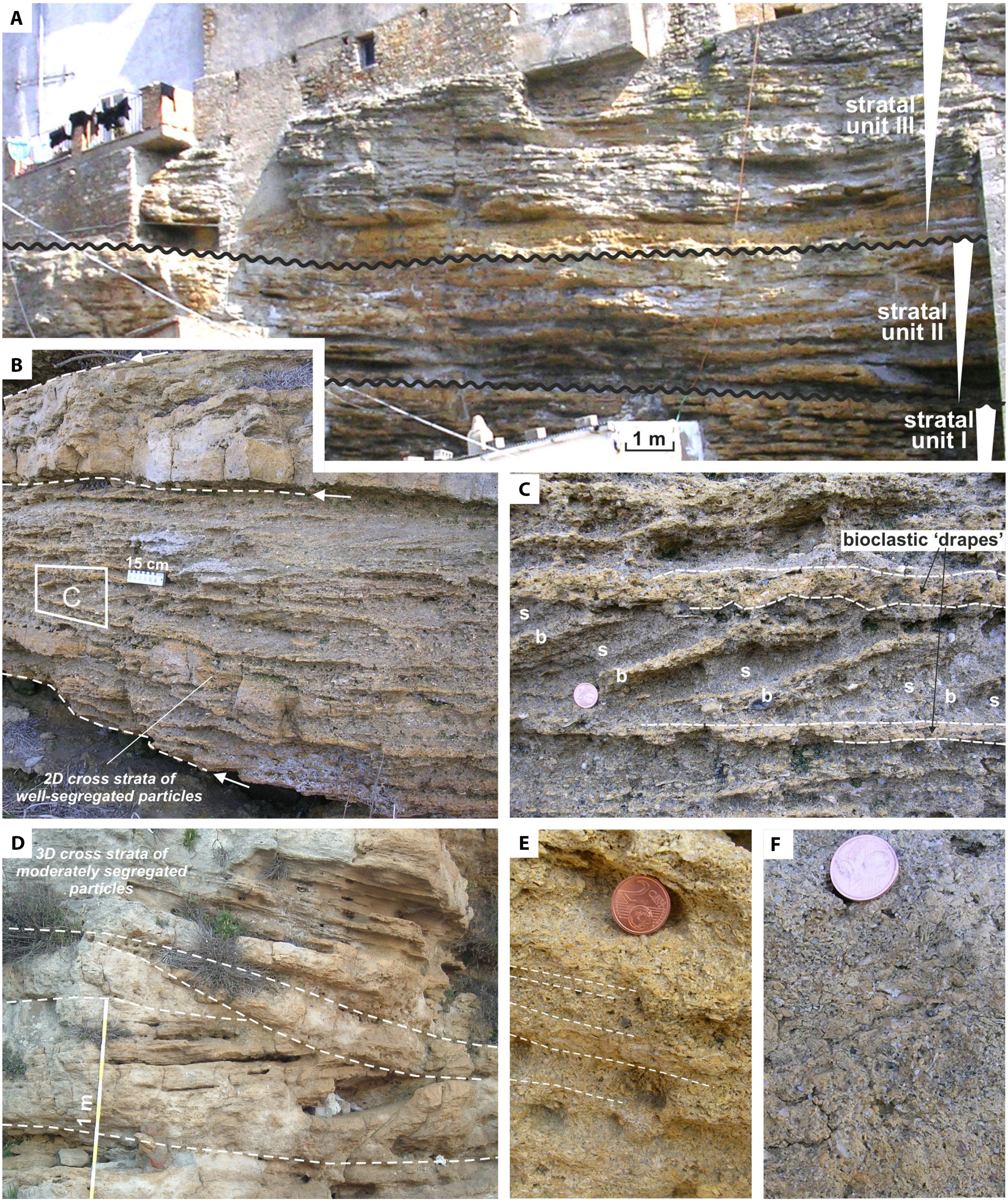

FIGURE 8 Outcrop exposure of the lower-middle Pliocene mixed tidalites in the Acerenza area. (A) Vertically-stacked mixed deposits showing the three stratal units (I, II and III) detected in the studied succession (from Chiarella & Longhitano, 2012). (B) 2D tidal cross-strata including neap/spring tidal cycles. Arrows point out the main discontinuity surfaces bounding cross-strata sets (C) Detail of foreset laminae forming semi-diurnal bundles of segregated bioclastic (*b*) and siliciclastic (*s*) intervals. Note the presence of bioclastic-rich 'drapes' bounding the base and the top of the cross-strata. (D) 3D cross-strata where mixed sediments show a moderate degree of heterolithic segregation. (E) Detail of internal heterogeneity of the previous facies. (F) Unsegregated mixed particles as observed in the topmost facies (coin used as scale in panels C, E and F is 2 cm in diameter).

facing the opposite direction also occur. Beds show scarce bioturbation.

These sediments pass upwards into an intermediate facies association, named (ii) 3D cross-strata of moderately-segregated particles (Figure 8D). The deposit consists of a mixture of medium to coarse-grained well-rounded siliciclastic sand admixed with bioclastic sands and granules. Sediments are organised into 3D cross-strata up to 80 cm thick. Bed bases are trough-shaped, forming elongated (elliptical) erosional scours filled by internal foreset strata (Figure 8D). Palaeocurrents are mostly unidirectional. The two heterolithic fractions show a lower degree of segregation when compared to the underlying facies (Chiarella & Longhitano, 2012; Figure 8E). Trough cross-strata are sparsely bioturbated with a low trace-fossil abundance. The ichnogenera recognised includes *Planolites* and *Skolithos* (Chiarella et al., 2012b). The upper part of each stratal unit is represented by the facies association named (iii) cross-strata of non-segregated particles. It consists of unsegregated siliciclastic and bioclastic particles with an abundant bioclastic fraction (Chiarella & Longhitano, 2012; Figure 8F). Sediments include very coarse sand-size and granule-size particles, arranged into 5–30 cm thick layers wedging-out landwards and gently dipping seawards, often amalgamated. Cross-strata sets show swales characterised by both low-angle (generally up to 10°) erosional surfaces and internal stratification, approximately parallel to the basal surface. Swaley cross-stratification (Figure 8D) exhibits a moderate degree of bioturbation related to the *Planolites* and *Skolithos* ichnogenera. Karstified beds are locally present showing vertical to sub-horizontal pipes forming irregular cylindrical cavities several decimetres in length (Chiarella & Longhitano, 2012).

In general, mixed deposits appear very well-cemented, except for stratigraphic bounding surfaces, which correspond to recessive horizons in outcrop.

3.3.2 | Depositional processes and environments

In the Acerenza mixed succession, the observed facies associations and their stratigraphic arrangements suggest deposition in a sublittoral coastal embayment (Chiarella et al., 2012a, 2012b, 2019).

Gravel and shell pavements are interpreted as a transgressive deposit following erosion and reworking of older sediments/rocks by ravinement processes. The overlying 2D cross-strata indicate an offshore-transition setting influenced by the action of traction currents in the lower flow regime and 2D flow conditions (Allen, 1968; Costello & Southard, 1981; Ashley, 1990; Southard & Boguchwal, 1990). The distinct segregation between siliciclastic and bioclastic foreset laminae occurring within the same cross-sets and at different scales suggests that sediment accumulation was controlled by cyclical variations in current energy possibly generated by tides (Chiarella & Longhitano, 2012).

The overlying 3D cross-strata record the migration of 3D dunes produced by higher velocity, but unstable, currents when compared to the flows responsible for the accumulation of the underlying 2D cross-strata. Flow instability is inferred by the frequent erosional scours separating individual cross beds, suggesting continuous interplay of tidal currents with shoaling waves in an intermediate shoreface environment (Chiarella & Longhitano, 2012).

The uppermost facies association of cross-strata of non-segregated particles represents accumulation in response to either strong oscillatory or combined unidirectional flows of variable energy in an upper shoreface environment (Chiarella & Longhitano, 2012; Chiarella et al., 2012b). Contrary to the underlying facies associations where segregation is markedly present, in this deposit, dominating waves neutralised the effect of tidal currents, inhibiting heterolithic sorting of mixed grains and, instead, producing a chaotic mixture of siliciclastic and bioclastic fragments (Chiarella & Longhitano, 2012).

4 | DISCUSSION

4.1 | Stratigraphic discontinuity surfaces in siliciclastic, carbonate and mixed siliciclastic-bioclastic tidalites: a qualitative assessment of their potential impact on fluid flow

In a reservoir characterisation framework, there are similarities and differences between siliciclastic, carbonate and mixed tidalites, both in their depositional characteristics and in the way in which they react to primary physical and chemical conditions which are crucial during subsequent, post-diagenesis fluid diffusion (Moore, 1989; Kupecz et al., 1997). For instance, high-energy versus low-energy tidal currents may generate terrigenous bedforms, which show overall similar architectures but, at close-up view, they may exhibit additional facies heterogeneities that result in highly-varying rock properties for internal fluid flows. In carbonate tidalites, the effects of syn-diagenetic to post-diagenetic solution and recrystallisation may greatly influence both sub-horizontal and sub-vertical permeability properties, especially in fine-grained, tabular carbonates. In mixed tidalites, the role of the heterolithic segregation between siliciclastic and bioclastic particles may result in different internal compartments with variable porosity and permeability properties.

These conditions, discussed in the following sections, are strongly influenced by the dimension (i.e. hierarchy scale), geometry and lateral continuity of the internal stratigraphic surfaces included in these three types of tidalites.

4.1.1 | High-energy versus low-energy siliciclastic tidalites

Siliciclastic tidalites are commonly composed of very well-sorted particles, because of the continuous process of sediment reworking by incoming and outgoing currents typified by discrete heterogeneities (layers) related to tidal cycles (Longhitano et al., 2012a). They also form heterolithic facies, due to the characteristic pulsation of the tidal energy that produces sandy deposits during high-energy phases and muddy interbeds during the lower-energy or slack-water phases of the tidal current (Reineck & Wunderlich, 1968; Reineck & Singh, 1980). This kind of stratigraphic architecture requires detailed and often complex numerical models at small to medium-scale to accurately represent the discrete lithofacies heterogeneity. These can be constructed using statistical techniques (Wen et al., 1998; Nordahl et al., 2005; Jackson et al., 2005; Ringrose et al., 2005; Nordahl & Ringrose, 2008). However, in many sub-tidal environments affected by high-energy tidal currents, mud is permanently kept in suspension with the resulting sedimentary deposit lacking fine-grained fractions (Longhitano & Nemec, 2005; Dalrymple, 2010). This architecture differs markedly from what is recorded in 'classical' tidal dune foreset deposits characterised by sand-mud couplets, which is considered an important source of heterogeneity in sandstone reservoirs (Weber, 1986; Weber & Van Geuns, 1990). Tidal cross-strata with tabular bounding surfaces form the elementary building blocks of many sandy deposits that accumulate in paralic and shallow-marine environments, such as tidal flats, estuaries and tidal sand ridges (Davis & Dalrymple, 2012). In these settings, tidal dune foresets, which can have 13–15% of mean porosity in subsurface reservoirs (Kupecz et al., 1997; Slatt, 2006; Messina et al., 2014), exhibit basal mud-rich bottomsets, often including back-flow ripples, which can be important permeability baffles if evaluated in a fluid-flow model (Massart et al., 2012). On the contrary, tidal foresets generated in higher-energy, marine settings, including tectonically-confined tidal straits (Longhitano, 2013), are generally characterised by no substantial grain-size changes between foreset and bottomset and a general lack of fine-grained sediment. Therefore, they represent sand bodies with better permeability properties and characterised by larger storage capacity, if compared to their lower-energy counterparts. However, in these tidal, mud-lacking deposits, pores can be greatly reduced during sediment compaction and early diagenesis, decreasing the fluid storage capacity of the bulk rock volume (Slatt, 2006). Consequently, fluids entrapped or migrating through the rock could have preferential pathways along discontinuity surfaces less affected by diagenetic cements.

A subsurface analogue for the siliciclastic tidalites presented in this paper is the Garn Formation (Kristine Field, North Sea; Quin et al., 2010). This sand-rich deposit, recently interpreted as a series of tidal sand ridges separated by wave-worked littoral facies (Messina et al., 2014), forms semi-isolated sandstone cross-strata sets which constitute up to 70% of the bulk formation thickness. The tidal sandstone ridges are encased in less permeable deposits and can be regarded as 'highly anisotropic permeability mini-containers'. This anisotropy derives from a complex combination of erosional and depositional surfaces that can increase the high permeability of such siliciclastic reservoirs (Messina et al., 2014). The combination of the different orders of surfaces might explain the rapid decline of reservoir pressure and low recovery factor observed during the appraisal stage of the prospect (Quin et al., 2010; Messina et al., 2014).

4.1.2 | The effects of solution and recrystallisation in peritidal carbonates

In peritidal carbonates, diagenetic processes may also generate an important reduction in primary porosity. Enos and Sawatsky (1981) documented the variable initial porosity of modern carbonate sediments (values ranging from 40 to 78%), and inferred that early diagenetic processes are responsible for the significant loss of preburial porosity (*ca* 20%) in analogous facies of nearby Pleistocene rocks. Budd et al. (1993) estimated that pre-compaction meteoric cements account for 3 to 37% of the volume in grainstones. However, Halley and Beach (1979) and Scholle and Halley (1985), based on studies of Holocene and Pleistocene sediments of Florida and the Bahamas, have claimed that porosity loss is slight during initial mineralogical stabilisation, but increases greatly during early cementation. Consequently, the main conduits for post-diagenetic fluid circulation are potentially concentrated in fault planes and fractures (when present) or, in the case of non-deformed rock volumes, in the main stratigraphic discontinuity surfaces.

Peritidal carbonate deposits, such as those documented in the Apulia Carbonate Platform, are mud-supported and have a low permeability since most pores correspond to unconnected intraskeletal chambers of bioclasts (mostly benthonic foraminifers), fenestrae and framework porosity (Moore, 1989). As in siliciclastic tidalites, diagenetic processes may generate an important reduction in carbonate porosity (Mazzullo, 2004). Alternatively, porosity can be significantly increased because of solution, recrystallisation and tectonic fracturing. This study disregards the effects of faulting and fracturing in reservoir rocks and only the consequences of solution and recrystallisation in peritidal carbonates will be discussed.

The most favourable process producing secondary porosity in peritidal carbonates is linked to relative sea-level drops that allow the exposure of carbonates to meteoric waters. Moreover, the establishment of a mixing water lens has been interpreted as a fundamental diagenetic modifier within both modern and ancient carbonate platforms (Melim et al., 2002; Baceta et al., 2007). As a result, the secondary porosity preferentially develops close to small-scale discontinuity surfaces at the top of peritidal sequences. Moulds, vugs or caverns may form when carbonates are dissolved by groundwater. The leaching of carbonates can be fabric selective (i.e. affects only aragonitic carbonate grains) or pervasive (i.e. affects all rock constituents and forms irregularly distributed vugs and caverns). In such a context, tidal pumping and tide-controlled groundwater-table fluctuations are effective mechanisms of pore water flow and, consequently, may actively contribute to decarbonation and to the growth of secondary porosity in peritidal carbonates during early diagenesis (Scholle & Ulmer-Scholle, 2003). Desiccation cracks and soil-forming processes also produce a significant textural change in peritidal carbonate facies. Clast-supported layers of intraclasts and black pebbles formed along discontinuity surfaces at the top of small-scale depositional sequences and palaeokarst breccias may affect reservoir porosity and may impart directional (sub-horizontal, preferentially) permeability improving reservoir performance characteristics (Ahr, 2008).

Discontinuity surfaces can also have a strong impact on reservoir compartmentalisation depending on their lateral extent and on the associated diagenesis of underlying rocks (Sattler et al., 2005).

An analogue oil field of the Apulia Cretaceous limestones described in the present study is represented by the Rospo di Mare Field in the central Adriatic Sea. This reservoir, located at a depth of 1310 m beneath a thick Plio-Quaterrnary mudstone sequence (André & Doulcet, 1991), consists of Lower Cretaceous peritidal deposits, belonging to the Apulia Carbonate Platform and accumulated in a depositional framework very similar to those of the coeval limestones presently exposed in the Murge area (see Figure 2C). The main oil reservoir is entrapped in secondary vugs and fractures enlarged by karstic dissolution after prolonged exposure of the platform. The karstified zones mostly developed horizontally, along primary flat bounding surfaces. Consequently, the production chiefly occurs along sub-horizontal wells.

4.1.3 | The role of heterolithic segregation in mixed tidalites

Mixed deposits are formed of sediments having both an extrabasinal (e.g. epiclastic or terrigenous) and intrabasinal (autochthonous to parautochthonous) component and more than 10% of their antithetic component (Chiarella & Longhitano, 2012; Chiarella et al., 2017). Similar to the high-energy siliciclastic tidal deposits described above, mixed tidalites of the Acerenza succession are generally mud-free. However, in mixed sediments, the lower density and platy shape of the bioclastic fraction play the same role as classical mud drapes in mud-rich siliciclastic tidalites (Longhitano, 2011; Chiarella & Longhitano, 2012). The hydraulic sorting exerted by tidally-modulated unidirectional currents is crucial for creating the resulting internal facies heterogeneities (Longhitano, 2011) and generates a 'spatial' distribution of the antithetic components (siliciclastic and bioclastic) in a mixed deposit, defined by different degrees of heterolithic segregation or 'segregation ratio' (Chiarella & Longhitano, 2012). The heterolithic segregation results in a partitioning of reservoir facies forming siliciclastic and bioclastic-rich foreset laminae with compartmentalised properties (see Figure 8C). Such variations in lithological composition translate into differential diagenetic cementation within laminae, and ultimately, to intra-lamina permeability changes. Mixed sediments are subject to more rapid and extensive porosity loss if compared to 'pure' siliciclastic tidalites, owing to the abundant bioclastic content, part of which can be quickly dissolved and re-precipitated during early diagenesis (Mansurbeg et al., 2009; Feng et al., 2013).

The antithetic dominance of one fraction over the other, which is a function of the primary hydraulic action of heterolithic segregation in mixed sediments and of relative base-level changes (Chiarella, 2011; Longhitano, 2011; Chiarella & Longhitano, 2012; Chiarella et al., 2012a, 2012b), can be observed in the studied section of Acerenza at different scales: (i) at strataset-scale, consisting of the progressive enrichment of bioclasts from the lowermost offshore-transition facies, upwards to the shoreface/beachface facies; (ii) at the strata-scale, where bioclasts, can be highly concentrated in lags or drapes intercalated with planar cross-strata (Figure 8C) where, on the contrary, siliciclasts and bioclasts are more 'balanced' in their proportions and variously segregated; (iii) at lamina-scale, where current-generated foresets show alternating bioclast-rich and siliciclast-rich tidal bundles.

These different facies characterised by such a heterolithic grain segregation are always separated by bounding surfaces (Figure 8B,D) which, generally, have a low cement content compared to the inter-surface bulk rock. Therefore, also in this case, depositional, erosional or pause planes may be the preferential conduits for fluid flow.

Although not always specifically described as 'mixed deposits', there are many case studies of reservoirs including mixed siliciclastic-bioclastic tidalites. One of the best-known mixed reservoirs is the Albian Lower Sendji Formation (N'Kossa Field; Offshore Congo) interpreted as a tidally-influenced, shallow-marine interval (Wonham et al., 2010). In this system, siliciclastic-bioclastic deposits have very heterogeneous reservoir properties, which cause highly varying vertical flow permeability changes. In particular, bioclastic-rich lamina-scale layers identified from well cores represent barriers to vertical fluid flow (Wonham et al., 2010), thus representing an important element to be detected at lamina to strata-scale. Moreover, large-scale (seismic to sub-seismic-scale) regressive and maximum flooding surfaces were described as defined by 0.5–5 m thick supratidal anhydritic-rich shale and tight micritic limestone deposits (Wonham et al., 2010). These extensive horizons work as barriers to vertical flow, causing rapid depletion of the main producing rock volumes and suggesting potentially more successful techniques of sub-horizontal hydrocarbon recovery.

4.2 | Scales of discontinuity surfaces and possible fluid pathways

The type of discontinuity surface bounding sediment bodies is strictly scale-dependent (Figure 9). Physical processes generating these surfaces have varying durations and magnitudes, which depend on the spatial scales at which they occur. For instance, to produce a discontinuity surface between two superimposed tidal bars, hundreds to thousands of years of tidal current interruption is required (e.g. the English Channel; Berné et al., 1988). On the contrary, similar discontinuities within a tidal bar may be generated by a sudden change in the dominant tidal current direction which occurs at shorter, monthly to annual, time scale (e.g. Cobequid Bay in the Bay of Fundy; Dalrymple et al., 1990). These two cases of discontinuities generated by processes acting at different temporal scale may result in surfaces with different properties. A long-lasting process of erosion or sediment starvation is often associated with settling or chemical precipitation of residual mineral components dissolved in marine waters, such as iron, zinc, sulphide and other minerals (Morad et al., 2013). This may result in mineralised coatings covering the discontinuity with a consequent reduction in porosity and permeability once this surface is subsequently buried by younger sediments. A short-term process of interruption and reprise of sedimentation in dune-bedded subtidal deposits may result, instead, in 'clean' stratigraphic discontinuities, becoming ideal planes for fluid-flow propagation, once preserved in a reservoir rock volume.

4.2.1 | Large (hectometre)-scale bounding surfaces

In strait-fill successions, large-scale, siliciclastic tidal cross-strata consist of sand sheets and sand ridges potentially reaching many hectometres in length and some tens of metres in thickness (Leva-Lopez et al., 2016; Chiarella et al., 2020; Longhitano et al., 2021). These lithosomes, which present architectural features similar to other tectonically-controlled current-dominated successions (e.g. the Baronia Formation, Olariu et al., 2012; Garn Formation, Messina et al., 2014; Rogn Formation, Chiarella et al., 2017) might represent the main subsurface reservoir, as it can be vertically-stacked and separated by mud-rich or less-permeable finer-grained inter-bodies related to relative sea-level changes (Messina et al., 2014; Figure 9A). The main bounding surfaces are basal and top discontinuities often characterised by a sharp lithological contrast with the overlying fine-grained deposits. These surfaces represent a major activation or slowing of the tidal currents flowing throughout the strait, due to a sudden change in basin oceanography (Anastas et al., 2006). The 2D and 3D reconstruction of these surfaces is crucial, because they express the overall geometry and sediment volume of the tidal lithosomes and, consequently, the resulting reservoir capacity (Messina et al., 2014). In the Catanzaro Strait (Figures 4A and 9A), the first case study used here, these surfaces are represented by basal discontinuities, often characterised by shell concentrations and mineralised pavements due to condensation or sediment starvation prior to sedimentation, and by topmost flat or undulating surfaces, which recorded the shape (lee to stoss profile) of large tidal bedforms at the moment of tidal current deactivation (Figure 9A).

In the peritidal limestones of the Apulia Carbonate Platform, large-scale sediment bodies are bounded by *ca* 5 to 20 m thick amalgamated and/or karstified intervals, rather than by distinct surfaces (Figure 9B). Three main bounding intervals have been recognised in the studied succession, all related to prolonged subaerial exposure phases, which correspond to important gaps in carbonate sedimentation. The first two bounding intervals capped by

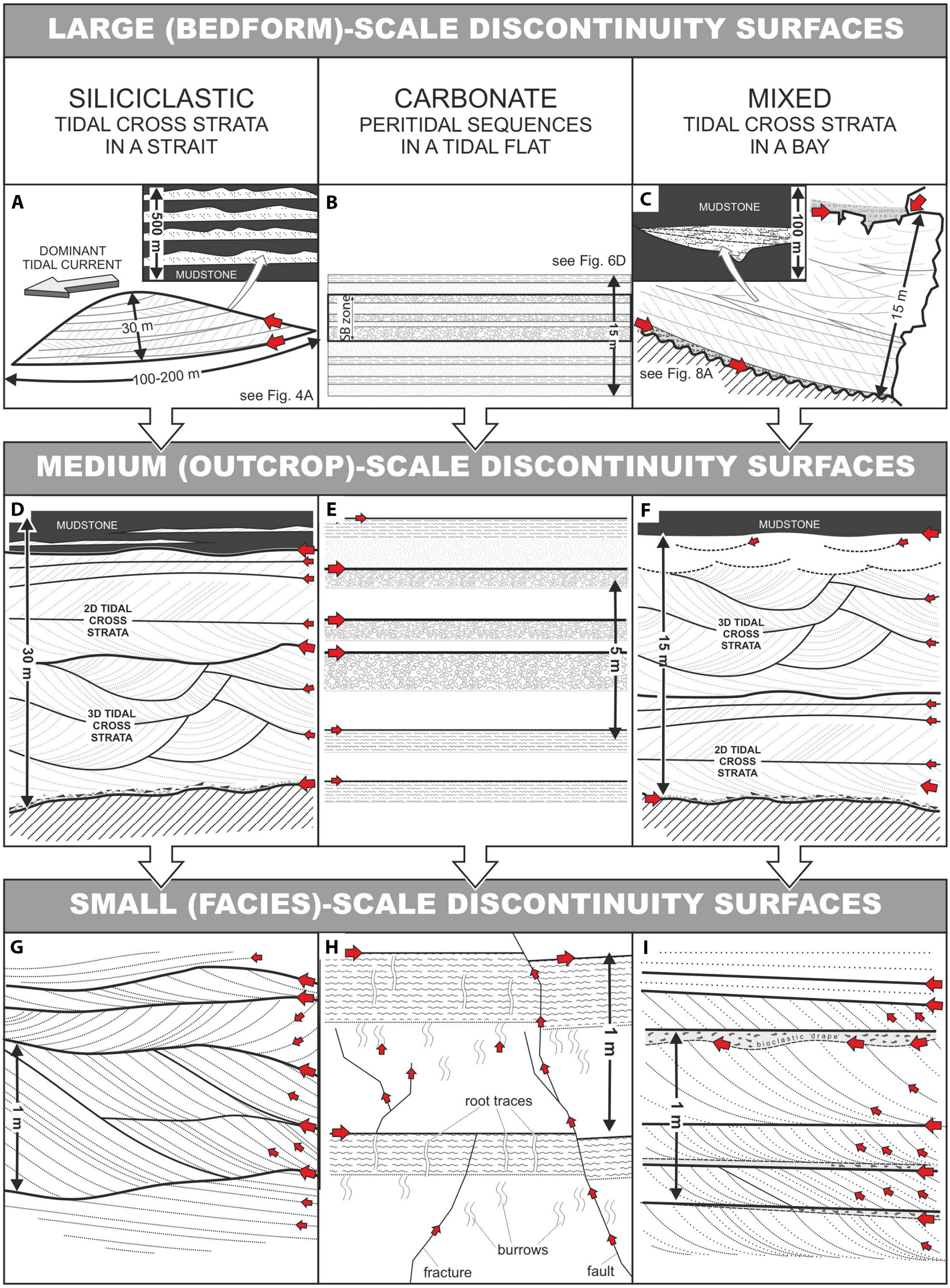

LARGE (BEDFORM)-SCALE DISCONTINUITY SURFACES
SILICICLASTIC
TIDAL CROSS STRATA IN A STRAIT
CARBONATE
PERITIDAL SEQUENCES IN A TIDAL FLAT
MIXED
TIDAL CROSS STRATA IN A BAY
A
500 m
DOMINANT TIDAL CURRENT
MUDSTONE
30 m
100-200 m
see Fig. 4A
B
see Fig. 6D
SB zone
15 m
C
MUDSTONE
100 m
15 m
see Fig. 8A
MEDIUM (OUTCROP)-SCALE DISCONTINUITY SURFACES
D
MUDSTONE
2D TIDAL CROSS STRATA
30 m
3D TIDAL CROSS STRATA
E
5 m
F
MUDSTONE
3D TIDAL CROSS STRATA
15 m
2D TIDAL CROSS STRATA
SMALL (FACIES)-SCALE DISCONTINUITY SURFACES
G
1 m
H
1 m
root traces
burrows
fracture
fault
I
bioclastic 'drape'
1 m

FIGURE 9 Comparison panel between siliciclastic, carbonate and mixed siliciclastic-bioclastic tidalites according to three descending-scale orders of internal heterogeneities. Possible fluid pathways are displayed by red arrows. (Arrows size indicates the relative scale of the potential conduits). (A) Siliciclastic tidalites form large-scale bedforms, which can be separated by offshore mudstone intervals if entirely preserved in the sedimentary record. (B) Carbonate tidalites form laterally extensive lithosomes consisting of vertically-stacked tabular strata. (C) Mixed tidalites show wedge-shaped geometry at decametre scale. These lithosomes can be encased in offshore fine-grained deposits when entirely preserved from erosion. (D) Metre-scale heterogeneities in siliciclastic tidal dunes consist of geometrically complex bounding surfaces in the lowermost part that become planar in the lowermost part of the succession. (E) In carbonate tidalites, the main possible ways for fluid internal propagation are those bounding the tops of each cycle (subaerial exposure surfaces). (F) In mixed tidalites, medium-scale discontinuity surfaces have generally planar geometry in the lowermost part but evolve to concave-up surfaces in the lowermost part. Note that, at the very top of the succession, bioclastic-rich, re-cemented intervals possibly inhibit any internal fluid circulation. (G) At facies scale, tidal cross-strata in non-porous siliciclastic sandstone show two types of discontinuities: (i) undulated, sub-horizontal surfaces bounding each cross-strata and (ii) internal foreset discontinuities. (H) In carbonate intertidal stromatolitic bindstone, the best surfaces for fluid internal propagation are the topmost ones. (I) In well-segregated, mixed tidalites, the preferential surfaces for fluid migration are instead inclined planes between foresets, with a low amount of bioclastic fraction, whereas bioclastic-rich intervals or 'drapes' act as deflectors for fluid transmission. In all these metre-scale examples, fluids move preferentially in a sub-horizontal direction.

palaeosol, *ca* 5–10 m thick (Figures 2D and 6D) are the result of condensed elementary sequences during a third order long-term sea-level fall. The third bounding interval corresponds to a *ca* 15–20 m thick collapsed dolomitic breccia (Figures 2D and 5A), which is interpreted as formed by pervasive meteoric dissolution of dolomitised beds. In this case, the record of small-scale depositional sequences was completely interrupted and the brecciation of dolomitic beds occurred as a result of the collapse of karstic cavities formed during a prolonged, probably tectonically enhanced, subaerial exposure phase (Spalluto, 2012). In the mixed sublittoral deposits of Acerenza, lithosomes form up to 45 m thick prograding wedges, internally subdivided into three stratal units, each up to 15 m thick (Chiarella, 2011; Chiarella & Longhitano, 2012; Chiarella et al., 2012b). Stratal units are separated by surfaces of marine flooding or angular unconformities that become surfaces of conformity basinwards (Figure 9C). Above these basal discontinuities, porous and permeable transgressive lag deposits enhance the likelihood of lateral fluid motion (Devine, 1991; Posamentier, 2002). The topmost surfaces of these units can also be surfaces of subaerial exposure, often incised and karstified. Consequently, fluids migrating along these surfaces may be characterised by complex pathways, which depend on the nature of the younger fill and the morphology of the karstified discontinuity that, often, may result in discontinuous 'pockets' or clusters of porous material which may inhibit sub-horizontal fluid-flow propagation.

4.2.2 | Medium (decametre)-scale bounding surfaces

In the lower Pleistocene siliciclastic succession of the Catanzaro Strait, poorly-sorted coarse-grained sands, with abundant granules and pebbles form 3D tidal cross-strata. These deposits pass laterally and upwards into well-sorted, medium-grained to coarse-grained sand organised into 2D tidal cross-strata (Chiarella, 2011; Longhitano et al., 2012c, 2012d). The uppermost interval consists of thinly-bedded, fine-grained sands evolving upwards into intensely-bioturbated silty-mudstones (Figure 9D). This vertically-stacked stratal pattern is interpreted as the response of the tidal strait to a virtually continuous decrease in the tidal current strength through time, due to the progressive enlargement of the strait cross-sectional area as consequence of a major relative sea-level rise (Chiarella, 2011; Longhitano et al., 2012c, 2014; Longhitano, 2013). In this transgressive succession, two groups of discontinuities can be distinguished (Figure 9D). The lowermost stratigraphic interval includes the first group of bounding surfaces representing the bases and tops of each individual 3D tidal cross-strata. These surfaces are erosional planes with concave-up or spoon-shaped geometry forming a trough or festoon cross stratification (Figure 9D). Upwards, the second group of surfaces are flat/planar gently-inclined (down-current) discontinuities. These surfaces are basal to 2D tidal cross-strata, migrating in one dominant direction or bi-directional (Figure 9D). Both 2D and 3D tidal cross-strata, and relative strata-bounding discontinuities, are interpreted as the result of a virtually continuous process of bedform migration within a large subtidal dune field, including sinuous and straight-crested, 3D and 2D tidal dunes (Chiarella, 2011; Chiarella et al., 2012a; Longhitano et al., 2014; Longhitano & Chiarella, 2020). This dune-bedded stratigraphic interval is capped at the top by a 10–20 m thick interval of rippled fine-grained sandstones and mudstones, which represents a potential stratigraphic top-seal from a reservoir perspective. Due to their lithological contrast, the above-described discontinuity surfaces might provide major pathways for fluid circulation in a subsurface porous container with such decametre-scale stratigraphic architecture, if internal sandy deposits had undergone cementation inhibiting vertical permeability. Consequently, fluids may virtually propagate through complex conduits in the lowermost trough cross-stratified interval, in both vertical and lateral directions if these surfaces have steep slopes. Within the overlying, planar cross-stratified interval, fluid pathways theoretically follow sub-horizontal or planar conduit surfaces, which favour the horizontal transfer of the bulk fluid volume. The vertical fluid migration is potentially prevented by the uppermost, low-permeability muddy interval, at this scale of observation.

In the Cretaceous peritidal limestones of the Apulia Carbonate Platform, the medium-scale bounding surfaces correspond to the top of small-scale and medium-scale sequences showing deeply penetrating meteoric diagenesis (Figure 9E). Usually, these sequences develop karstic solution cavities and/or calcrete horizons. The development of these surfaces is linked to relative fall in sea level that exposed the platform for long enough to produce a deep diagenetic modification of peritidal carbonates in subaerial environments. According to many authors (see D'Argenio et al., 2004; Strasser et al., 1999), these bounding surfaces record the end of eccentricity cycles, either of short (*ca* 100 kyr) or long (*ca* 400 kyr) duration.

The occurrence of mud cracks, breccia layers and early-diagenetic, solution-enlarged pores and fractures at the top of these sequences may significantly increase the porosity and permeability of tidal carbonates, although the late burial diagenesis may induce the opposite process by the precipitation of calcite cements, which partly or totally occlude pores and fractures. Despite this, medium-scale discontinuity surfaces may potentially represent important conduits for fluids migrating in carbonate deposits formed in peritidal environments.

In the middle Pliocene mixed deposits of Acerenza, tidalites form well-segregated 2D cross-strata passing upwards to moderately-segregated 3D cross-strata (Chiarella, 2011; Chiarella & Longhitano, 2012; Chiarella et al., 2012b) (Figure 9E). This vertical facies trend is interpreted to be the result of transition from a tide-influenced to a wave-dominated, sublittoral environment due to a normal regression phase, with consequent upward-increasing bed shear stress (Chiarella & Longhitano, 2012). In this regressive sequence, the main bounding surfaces are grouped into two categories of discontinuities based on their distinctive geometries (Figure 9E). The lowermost surfaces bounding 2D cross-strata are generally flat and sub-horizontal, representing bed bottoms and tops. The uppermost surfaces consist of elongated elliptical erosional scours bounding 3D cross-strata. This interval passes upwards into swaley cross-strata, characterised by the high carbonate fraction (bioclasts *ca* 80%) (Chiarella & Longhitano, 2012). In such a vertical sequence, fluid pathways might have sub-horizontal or planar conduits in the lowermost interval, with a preferential horizontal migration. Within the overlying interval, fluid migration may follow more complex conduits in both lateral and vertical directions (Figure 9E). For this reason, the main stratal surfaces might be the preferred possible conduits for fluids migrating within the studied mixed tidalites.

4.2.3 | Small (metre)-scale bounding surfaces

Metre-scale bounding surfaces in tidalites are readily detectable features in outcrop but can be difficult to disentangle in well core stratigraphic records. However, smaller-scale, microscopic characteristics also have an important role in affecting permeability and can be evaluated to determine their effect on the intra-stratification heterogeneities that ultimately define fluid transmission in tidalites (Blatt et al., 1980; Chandler et al., 1989). Nevertheless, this scale of observation remains beyond the scope of this paper.

Siliciclastic tidal cross-strata documented in the Catanzaro Strait-fill deposits show a variety of internal, metre-scale discontinuity surfaces. Across a section parallel to the dominant sand transport, these surfaces are dune lee sides, where grain avalanching produce a forward accretion of the bedform, and reactivation surfaces (Figure 9G). The overall geometry of these discontinuities is generally tabular, even though they may exhibit a concave or complex shape in 3D tidal cross-strata dominantly inclined toward the major current direction.

In the Cretaceous Apulia carbonate tidalites, small-scale surfaces capable of internally conveying fluids (Figure 9H) are observable at the top of small-scale sequences including intertidal and supratidal environments. These surfaces show only ephemeral evidence of subaerial exposure. Usually, a few laminoid fenestrae a few millimetres in extent are the most common feature that characterise tidally-laminated dolomitic limestones lying immediately below these surfaces, as well as the occurrence of small mud cracks and other microkarstic features observable only in thin section. According to many authors (D'Argenio et al., 1999, 2004; Strasser et al., 1999), these bounding surfaces may form at the end of orbital precession cycles (*ca* 20 kyr), preserving evidence of only short subaerial exposure periods. Usually, mud-supported tidal carbonates formed at the top of small-scale depositional sequences are not considered important conduits for fluid migration since they mostly develop unconnected pores, which are partially or completely filled by late calcite cements. However, since diagenesis is not a one-way process, the replacement of micrite by dolomite crystals might significantly increase the porosity and permeability of these carbonates.

Small, metre-scale reservoir properties of mixed tidal cross-strata documented in the Acerenza palaeobay-fill strata are strictly related to the antithetic percentage of siliciclastic and carbonate grains. In particular, (i) the heterolithic composition controls the final texture of the deposits, (ii) different grain shapes between siliciclastic (spherical) and bioclastic (platy) particles impacts the porosity (Payton et al., 2022b), (iii) changes in primary and secondary porosity are controlled by the occurrence of carbonate grains mixed with the siliciclastic grains (Mansurbeg et al., 2009; Feng et al., 2013). In the Acerenza cross-strata, tidally-modulated subaqueous water flows acted as the principal factor in segregating particles, separating coarser and lighter bioclastic grains from finer and heavier siliciclastic grains. This major mechanism, dominating the offshore-transition and lower shoreface environments, typically resulted in siliciclastic-bioclastic bundles within individual cross-strata (Longhitano, 2011; Chiarella & Longhitano, 2012; Chiarella et al., 2012b; Longhitano et al., 2012b). As it is common in pure siliciclastic settings, this hydraulic sorting generates distinct lateral changes in grain size that ultimately produces sub-horizontal differences in reservoir potential. Hydraulic sorting results in a partitioning of the reservoir facies forming siliciclastic and bioclastic-rich foreset laminae with different properties. Such variations in grain composition are probably translated into differential dissolution and cementation within laminae, and finally, into lamina-scale permeability variations. Foresets act as mini-compartments separated by high-angle stratal truncations, textural differences and permeability baffles (Messina & Nemec, 2006; Longhitano, 2011; Messina et al., 2014). In the mixed deposits of Acerenza, more cemented carbonate-rich laminae act as baffles to sub-horizontal fluid flows (Figure 9I). Cementation in mixed deposits is enhanced by the presence of abundant carbonate grains, which can act as source of carbonate ions and as nuclei for precipitation and growth of carbonate cement (Mansurberg et al., 2009).

4.3 | Reservoir heterogeneity in siliciclastics, carbonates and mixed tidalites

Many sedimentary reservoirs are characterised by a significant loss of primary porosity due to their deep burial (Bjørlykke et al., 1986; Paxton et al., 2002), and resulting reduction of inter-granular pore spaces with depth (Halley & Schmoker, 1983). This condition is more frequent, for instance, in structureless or massive sandstone deposits (Meyer, 2002). However, if deposits are extremely tight, and sediments are organised into discontinuity-bounded lithosomes and/or strata, including internal planes of different scales (e.g. strata-sets, strata, laminae, etc.), these surfaces might work as preferential paths, balancing the effect of loss of primary porosity due to compaction.

Brandsæter et al. (2001) argued that the ratio between vertical and horizontal permeability (Kv/Kh ratio) is one of the most important parameters influencing fluid movement in a sedimentary deposit. However, in tidal strata fluids have a dominant horizontal component if moving along the main bounding strata surfaces (Figure 10A,B), with a consequent $Kh>>Kv$ (Massart et al., 2016a, 2016b). On the contrary, if bounding strata surfaces are occluded by cement or fine-grained sediment, discontinuity surfaces of lower hierarchical order are the preferential conduits (Jackson et al., 2005). Consequently, in both siliciclastic, carbonate and mixed tidal cross-strata, fluids move along internal foreset (conformable) surfaces, which might have angular or tangential geometry (Figure 8). Fluid transport still prevails along the horizontal, but with a minimal vertical component ($Kh>Kv$) (Figure 10A).

In this framework, the dominance of uni-directional or bi-directional tidal cross-strata is of crucial importance. In uni-directional tidal cross-strata, fluids are expected to preferentially 'climb' foreset surfaces and migrate updip (as opposed to the tidal foreset dip). This condition may generate significant fluid motion in a particular direction contrary to the original bedload transport. In bidirectional tidal cross-strata, the preferential pathway of fluid migration thus depends upon the dominant palaeocurrents or the thickness of the prevailing tidal foreset. Thus, the variation between vertical (ΔKv) and horizontal (ΔKh) permeability is strongly conditioned by the internal heterogeneity of the tidal cross-strata.

In peritidal carbonates, the subaerial or subaqueous origin of the main bounding surfaces, their lateral extent and the early diagenetic history of underlying peritidal limestones (see discussion in the previous sections) are key in their subsequent role for fluid movements (Eltom et al., 2020). After lithification, that surfaces originated in subtidal conditions become conduits along which the possible horizontal movement of fluids (Kh) is dominant to their vertical component (Kv), because of the prevalence of sub-horizontal flat-shaped geometries. These planes are often opened (Figure 10B) because post-depositional desiccation and contraction can greatly reduce the volume of the carbonate mud favouring the storage of significant amounts of fluids. In cases where surfaces originated in inter-tidal and supra-tidal environments, post-depositional subaerial exposure favoured carbonate mud desiccation and consequent cracking, which in section view appear as sub-vertical fractures. These fractures, associated with vertical burrows, may link sub-horizontal surfaces acting as connectors and favouring, at times, the vertical transfer of fluids (Figure 10B).

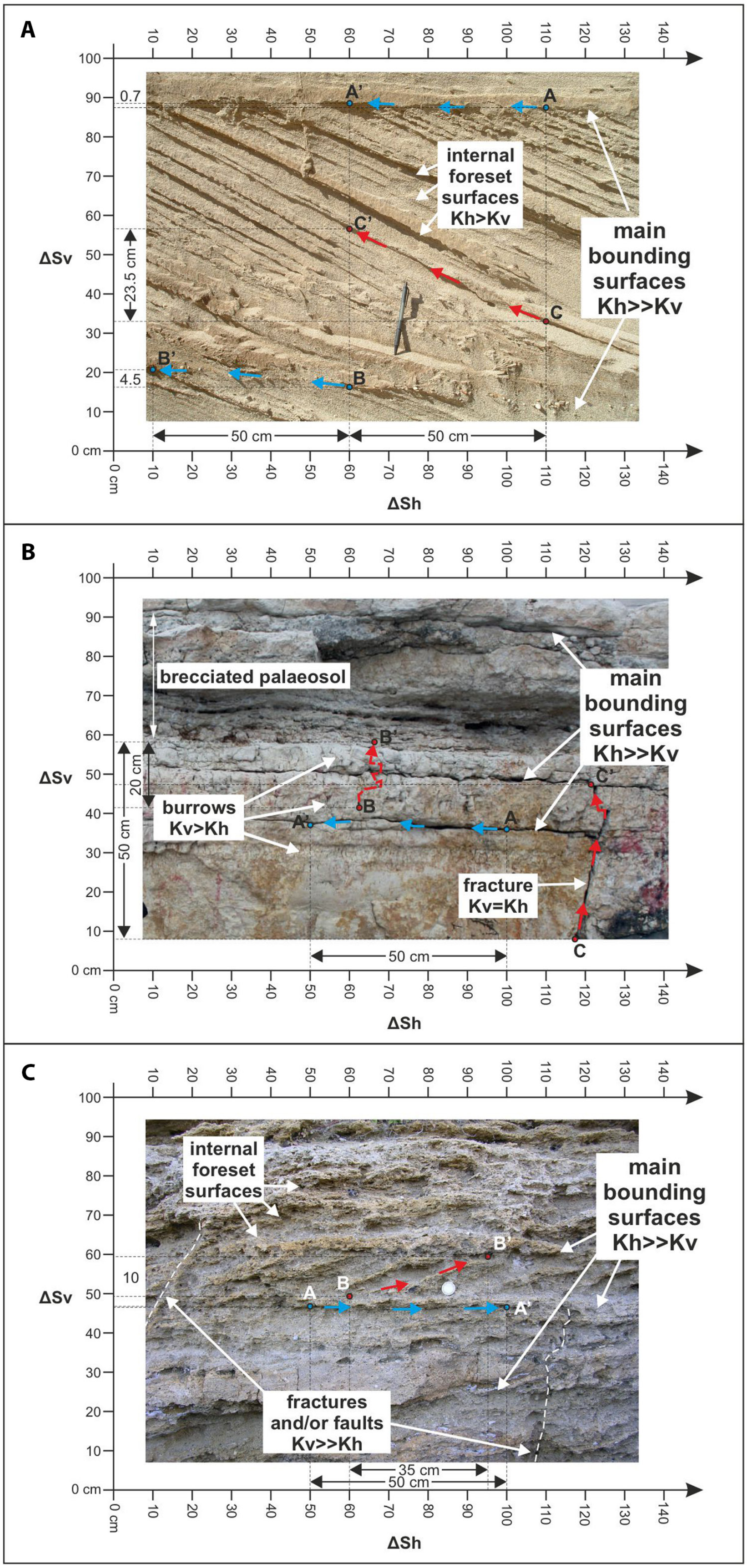

FIGURE 10 2D tidalite sections where the possible fluid pathways along internal discontinuities are hypothetically reconstructed with the estimation of the amount of sub-vertical (Δ*Sv*) and sub-horizontal (Δ*Sh*) movement. (A) In siliciclastic tidal cross-strata, fluids may migrate along the main bounding strata surfaces, following mainly sub-horizontal pathways (A to A′ and B to B′). In these cases, the horizontal permeability (*Kh*) can be considered slightly larger than vertical permeability (*Kv*). Alternatively, internal foreset surfaces may deflect fluid migration, with a low amount of sub-vertical movement. (B) Carbonate tidal flat facies allow preferential sub-horizontal fluid migration along the main bounding strata surfaces (A to A′), except in case of presence sub-vertical burrows or fractures which, acting as vertical conduits, enhance locally Kv (B to B′ and C to C′). (C) In mixed tidal cross-strata, where the internal heterolithic segregation separates bioclastic—from siliciclastic-rich intervals, fluids can migrate sub-horizontally (A to A′) along the main strata surfaces. In case of the presence of bioclastic baffles, fluids propagate along siliciclastic-rich foreset surfaces. In both conditions *Kh* is always greater than *Kv*.

Mixed siliciclastic-bioclastic cross stratified sandstones have very similar internal stratal architecture compared to the siliciclastic tidalites described in this paper (Figure 10C). Fluid pathways can be predicted by reconstructing the same geometrical relationships discussed for siliciclastic cross-strata. However, the presence of bioclastic-rich interstrata or drapes between cross-strata (Figure 8C) enhances the dominance of the sub-horizontal over the sub-vertical permeability (Figure 10C) ($Kh >> Kv$). This is due to the early cementation that bioclasts produce when concentrated in distinct layers, which result in sub-horizontal permeability baffles. Fluids are thus 'entrapped' in such laterally-elongated compartments and can transfer to the uppermost strata only if these bioclastic intervals have limited lateral extension or in the presence of sub-vertical (semi-opened) fractures and/or faults (Figure 10C).

Primary porosity can be significantly high (up to 20–25%) in many tidal deposits although they are deeply buried (Meyer & Krause, 2001; Burton & Wood, 2011). In this case, either sub-horizontal or sub-vertical permeabilities are usually related to inter-granular primary porosity, but their vectorial component can be strongly conditioned if internal discontinuity surfaces occur, resulting in specific fluid flow pathways (Figure 11).

In siliciclastic, cross-stratified mud-free sandstones including foresets with tidal bundles (i.e. alternating coarse-grained and finer-grained lamina-sets), both sub-horizontal (Kh) and sub-vertical (Kv) permeability result from the sum of the inter-granular pore transmissivity properties measured along coarse-grained and fine-grained intervals (Figure 11A). The resulting fluid flow derives from a combination of horizontal and vertical porosity features, but its vector (i.e. space orientation) can be strongly conditioned by the orientation of the internal foreset conformity surfaces (Figure 11A). Even at this scale of observation, the resultant fluid pathways follow along the main discontinuities of a 'surface-induced' permeability (Figure 11A).

In tidal flat carbonates, Kh is always dominant over Kv (Figure 11B), except where the presence of vertical burrows, cracks or root traces may locally enhance fluid transmission upwards. However, supra-tidal and intertidal mudstones can also exhibit primary porosity, even though they are generally characterised by low values (Major & Holtz, 1997). Sub-horizontal bounding surfaces thus control the overall internal fluid pathways, whose vectorial component can be expected to have a dominant sub-horizontal direction but one influenced by subordinate vertical deviation (Figure 11B).

In mixed siliciclastic-bioclastic tidal cross-strata, interstratal bioclastic 'drapes' (usually representing permeability baffles due to their early cementation), may control the resultant sub-surface permeability (Figure 11C). Foreset laminae can have very different internal porosity, due to their heterolithic component fractions, which result in highly-variable, inter-particle degrees of cementation. However, foreset conformity surfaces may provide the primary internal fluid flow paths, which might subsequently be deflected by bioclastic seals (Figure 11C). Therefore, in mixed siliciclastic-bioclastic reservoirs, fluids are forced to flow with a dominant sub-horizontal direction, but one

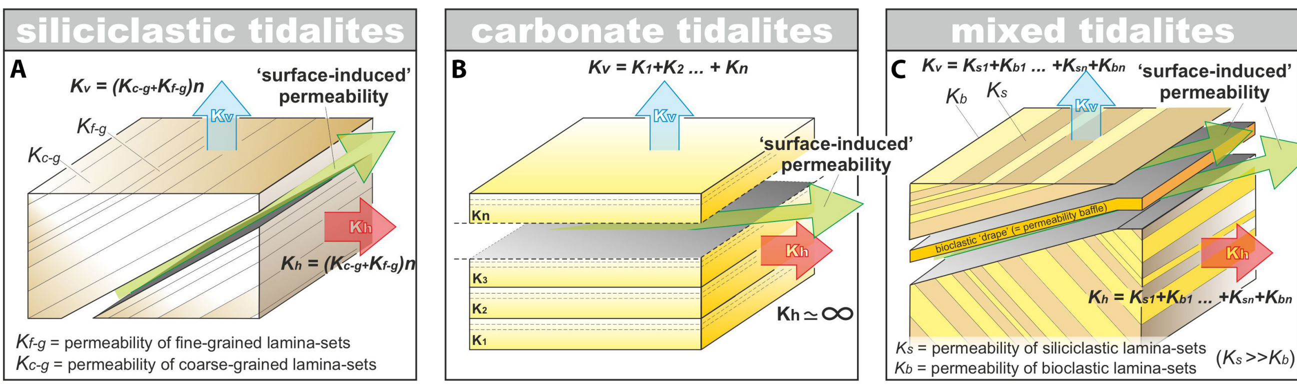

FIGURE 11 Surface-based models predicted for siliciclastic, and mixed tidal deposits in case of significant primary porosity. (A) In cross-stratified tidal sandstones, both sub-horizontal and sub-vertical permeability result from the sum of the porosity evaluated through coarse- and fine-grained lamina-sets (tidal bundles). However, the preferential direction for internal fluids is conditioned by the inclined conformity surfaces forming tidal foreset. The 'surface-induced' permeability has thus a vector of propagation parallel to the master surfaces. (B) Carbonate tidalites have a dominant sub-horizontal permeability deriving from the lateral extension of the flat sub-horizontal master surfaces. However, internal porosity may favour subordinate vertical fluid movement, influencing the resultant space orientation of the total permeability. (C) In mixed tidal cross-strata, fluids move both sub-horizontally and sub-vertically in case of relevant porosity. However, bioclastic drapes, usually occupying the top of the cross-strata (see Figure 8C), work as permeability baffles, influencing the final 'surface-induced' porosity.

which is strongly influenced by the geometry and orientation of local bioclastic-rich intervals.

5 | CONCLUSIONS

Tidalites documented in siliciclastic, carbonate and mixed siliciclastic-bioclastic deposits from southern Italy were reviewed and compared, with the major aim to detect hierarchies of bounding surfaces significant for internal fluid migration pathways. Although these ancient deposits accumulated in microtidal settings, the chosen examples recorded tide-dominated and tide-influenced environments in a tide-dominated palaeo-strait, a peritidal platform and in a tide-influenced palaeo-bay.

It is assumed that the considered examples of tidalites show internal textures that greatly reduced primary porosity during compaction and after diagenesis, so that eventual propagating fluids or gas have preferential conduits along the main discontinuity surfaces, both erosional and depositional.

Stratigraphic surfaces were thus described according to their hierarchical orders of descendant dimension, from hectometre, to decametre, to metres-scale of observation.

In siliciclastic sandstone dune-bedded complexes deposited in a tidal strait, large-scale surfaces, which can have comparable dimensions to seismic-scale reflectors documented in similar successions, coincide with basal transgressive flat planes in which the concentration and mineralisation of the fossil remains, due to case hardening processes typical of long-lasting sediment starvation, inhibit fluid migration. On the contrary, the top surfaces of these tidal dunes, represented by a sharp lithological contrast with the overlying offshore mudstone, are undulatory planes ideal for sub-horizontal fluid transfer or entrapment. In particular, compound-dune crests lying in an analogue stratigraphic setting, if thus adequately preserved by processes of post depositional erosion and/or draping by muddy deposits, are suggested to host mini-reservoirs or compartments that should be evaluated in similar subsurface settings.

Tidal flat carbonates exhibit large-scale surfaces consisting of flat planes extending over hundreds of metres, along which fluid can be transferred horizontally, with limited vertical movement, except for the presence of local interconnections due to sub-vertical faults or fractures.

In bay-fill mixed deposits, basal surfaces are transgressive horizons where, also for this example, fluid transmission can be inhibited because of the presence of well-cemented thick gravel/shell lags. On the contrary, surfaces related to subaerial exposures and incision offer complex planes for fluid migration, with the transmission rate depending upon the grain size and cementation of the overlying fill.

At medium scale, strait-filling lithosomes form deepening-upward, tens of metres thick strata-sets, including 3D to 2D tidal cross-strata overlain by offshore mudstone. The main surfaces detectable at this scale are complex concave-up discontinuities in the lowermost part that evolves to sub-horizontal planes in the uppermost part. Along these surfaces, fluids potentially migrate with horizontal directions predominant. In tidal flat carbonates, also at this scale, fluids are forced to move sub-horizontally, since discontinuity surfaces are located at the top of tabular peritidal sequences. In addition, the occurrence of brecciated palaeosols, mud cracks, vertical-oriented root traces and burrows also induces secondary vertical pathways for internal fluids, increasing greatly the eventual internal fluid pressure. Mixed, siliciclastic-bioclastic 8–15 m thick packages contain vertically-stacked 2D to 3D cross-strata. This recurrent sequence is associated with an upward decrease in the degree of heterolithic segregation between siliciclastic and bioclastic particles and an increase in the carbonate content. Fluids migrating at this outcrop-scale in mixed tidalites may thus follow sub-horizontal pathways in the lowermost part, passing to complex sub-horizontal and vertical directions upwards. Fluid mobility may be inhibited in the uppermost part of these tidal sequences, due to 'pavements' of carbonate precipitates and consequent cementation, occluding primary depositional or erosional surface conduits.

Stratigraphic surfaces in siliciclastic tidal cross-strata considered at small (metre) scale mostly consist of inclined (foreset) planes, which can transmit fluids with the amount of sub-horizontal transfer exceeding the amount of sub-vertical movement. In carbonate tidal flat facies, sub-horizontal depositional surfaces are, also at this scale, preferential conduits, although vertical primary cracks, roots and burrows, can also favour vertical propagation of internal fluids. Mixed tidalites considered at centimetre-scale, show good horizontal transfer potential that can be reduced by the presence of internal permeability seals, due to local concentration of bioclast-rich drapes accumulated during tidal slack-water stages.

In all three considered examples of this surface-based study on the reservoir potential of siliciclastic, carbonate and mixed tidalites, fluids may always have preferential sub-horizontal components of movement if transmitted through the main discontinuity surfaces of different scales or hierarchies. This condition may also be valid in case of significant primary porosity because internal discontinuity planes favour a 'surface-induced' permeability.

Understanding the nature, geometry and possible 3D-extension of internal discontinuity surfaces in stratified sedimentary rocks is thus a key challenge to predict their sub-horizontal permeability *Kh* which, based on the considerations presented in this study, might be two or three orders of dimension greater than the sub-vertical permeability *Kv*.

ACKNOWLEDGEMENTS

An early version of this paper benefited of comments provided by A. Strasser and R.J. Steel. Thanks to Valentina M. Rossi, Robert W. Dalrymple and an anonymous reviewer for their help in improving the manuscript.

FUNDING INFORMATION

DC research is supported by the Clastic Sedimentology Investigation Group. SGL was supported by the University of Basilicata (grant no. 432/2012).

CONFLICT OF INTEREST STATEMENT

The authors declare that they have no known competing financial interests or personal relationships that could have appeared to influence the work reported in this paper.

DATA AVAILABILITY STATEMENT

Data sharing not applicable to this article.

ORCID

Domenico Chiarella https://orcid.org/0000-0003-2482-0081
Sergio G. Longhitano https://orcid.org/0000-0003-4978-4582
Luigi Spalluto https://orcid.org/0000-0001-9439-6461

REFERENCES

Agar, S.S.M. & Geiger, S. (2015) Fundamental controls on fluid flow in carbonates: current workflows to emerging technologies. *Geological Society of London, Special Publication*, 406, 1–59.

Ahr, W.M. (2008) Geology of carbonate reservoirs. In: *The identification, description, and characterization of hydrocarbon reservoirs in carbonate rocks*. John Wiley and Sons, Inc, p. 277. https://doi.org/10.1002/9780470370650

Aker, E., Kjønsberg, H., Fawad, M. & Haque Mondol, N. (2021) Estimation of thickness and layering of Johansen and Cook sandstone at the potential CO_2 storage site Aurora, Trondheim conference on CO_2 Sotrage, 21–23 June, Trondheim, Norway.

Aker, E., Bjørnaråa, T., Braathenb, A., Brandvollc, Ø., Dahled, H., Nordbottend, J.M., Aagaarde, P., Hellevange, H., Alemue, B.L., Phame, V.T.H., Johansenc, H., Wangenc, M., Nøttvedtf, A., Aavatsmarkg, I., Johannessend, T. & Durandh, D. (2011) SUCCESS: sUbsurface CO_2 storage—critical elements and superior strategy. *Energy Procedia*, 4, 6117–6124.

Allen, J.R.L. (1968) *Current ripples*. Amsterdam: North Holland Publishing Company, p. 433.

Alshakri, J., Hampson, G.J., Jacquemyn, C., Jackson, M.D., Petrovskyy, D., Geiger, S., Machado Silva, J.D., Judice, S., Rahman, F. & Costa Sousa, M. (2023) A screening assessment of the impact of sedimentological heterogeneity on CO_2 migration and stratigraphic-baffling potential: sherwood and Bunter sandstones, UK. *Geological Society, London, Special Publications*, 528(1), 245–266. https://doi.org/10.1144/sp528-2022-34

Ambrose, W., Lakshminarasimhan, S., Holtz, M., Nuenẽz-López, V., Hovorka, S.D. & Duncan, I. (2008) Geologic factors controlling CO_2 storage capacity and permanence: case studies based on experience with heterogeneity in oil and gas reservoirs applied to CO_2 storage. *Environmental Geology*, 54, 1619–1633.

Anastas, A.S., Dalrymple, R.W., James, N.P. & Campbell, S.N. (2006) Lithofacies and dynamics of a cool-water carbonate seaway: mid-Tertiary, Te Kuiti Group, New Zealand. In: Pedley, H.M., Carannante, G. (Eds.) *Cool-water carbonates: depositional systems and palaeoenvironmental controls*. Geological Society of London Special Publication, 255, 245–268.

André, P. & Doulcet, A. (1991) Rospo Mare Field-Italy Apulian Platform, Adriatic Sea. In: Foster, N.H. & Beaumont, E.A. (Eds.) *Stratigraphic traps II*. Los Angeles: AAPG Treatise of Petroleum Geology, pp. 29–54.

Araújo, L.B., Rustichelli, B., Xavier, A. & Barbosa, A. (2021) Structural and sedimentary discontinuities control the generation of karst dissolution cavities in a carbonate sequence, Potiguar Basin, Brazil. *Marine and Petroleum Geology*, 123, 104753.

Ashley, G. (1990) Classification of large-scale subaqueous bedforms: a new look at an old problem. *Journal of Sedimentary Petrology*, 60, 160–172.

Baceta, J.I., Wright, V.P., Beavington-Penney, S.J. & Pujalte, V. (2007) Palaeohydrogeological control of palaeokarst macroporosity genesis during a major sea-level lowstand: Danian of the Urbasa–Andia plateau, Navarra, North Spain. *Sedimentary Geology*, 199, 141–169.

Benson, S.M., Bickle, M., Boon, M., Haese, R., Kurtev, K., Matthai, S., Neufeld, J., Watson, M. & Winkelman, G. (2018) Quantifying the impact of heterogeneity on CO_2 migration and trapping in saline aquifers, 14th International Conference on Greenhouse Gas Control Technologies, 21–25 October, Melbourne, Australia.

Berné, S., Auffret, J.P. & Walker, P. (1988) Internal structure of subtidal sandwaves revealed by high-resolution seismic reflection. *Sedimentology*, 35, 5–20.

Blatt, H., Middelton, G. & Murray, R. (1980) *The origin of sedimentary rocks*, 2nd edition. New York: Prentice-Hall, p. 782.

Bjørlykke, K., Aagaard, P., Dypvik, H., Hastings, D.S. & Harper, A.S. (1986) Diagenesis and reservoir properties of Jurassic sandstones from the Haltenbanken area, offshore mid-Norway. In: Spencer, A.M., Campbell, C.J., Hanslien, S.H., Holter, E., Nelson, P.H.H., Nysather, E. & Ormaasen, E.G. (Eds.) *Habitat of hydrocarbons on the Norwegian continental shelf. Norwegian Petroleum Society Proceedings*. London: Graham and Trotman, pp. 275–286.

Brandsæter, I., Wist, H.T., Næss, A., Lia, O., Arntzen, O.J., Ringrose, P.S., Martinius, A.W. & Lerdahl, T.R. (2001) Ranking of stochastic realizations of complex tidal reservoirs using streamline simulation criteria. *Petroleum Geoscience*, 7, 53–63.

Budd, D.A., Hammes, U. & Vacher, H.L. (1993) Calcite cementation in the upper Floridan aquifer: a modern example for confined-aquifer cementation models? *Geology*, 21, 33–36.

Burton, D. & Wood, L.J. (2011) Geologically-based permeability anisotropy estimates for tidally-influenced reservoirs using quantitative shale data. *Petroleum Geoscience*, 19, 3–20.

Casteleyn, L., Robion, P., Collin, P.-Y., Menéndez, B., David, C., Desaubliaux, G., Fernandes, N., Dreux, R., Badiner, G., Brosse, E. & Rigollet, C. (2010) Interrelations of the petrophysical, sedimentological and microstructural properties of the Oolithe

Blanche Formation (Bathonian, saline aquifer of the Paris Basin). *Sedimentary Geology*, 230(3–4), 123–138. https://doi.org/10.1016/j.sedgeo.2010.07.003

Chandler, M.A., Kocurek, G., Goggin, D.J. & Lake, L.W. (1989) Effects of stratigraphic heterogeneity on permeability in Eolian sandstone sequence, Page sandstone, northern Arizona. *AAPG Bulletin*, 73, 658–668.

Chandra, V., Barnett, A., Corbett, P., Geiger, S., Wright, P., Steele, R. & Milroy, P. (2015) Effective integration of reservoir rock-typing and simulation using near-wellbore upscaling. *Marine and Petroleum Geology*, 67, 307–326.

Chiarella, D. (2011) Sedimentology of Pliocene–Pleistocene mixed (lithoclastic–bioclastic) deposits in southern Italy (Lucanian Apennine and Calabrian Arc): depositional processes and palaeogeographic frameworks. PhD Thesis, University of Basilicata, Potenza, 216 p.

Chiarella, D. (2016) Angular and tangential toeset geometry in tidal cross-strata. *Contributions to Modern and Ancient Tidal Sedimentology*, 191–201. https://doi.org/10.1002/9781119218395.ch10

Chiarella, D., Capella, W., Longhitano, S.G. & Muto, F. (2021) Fault-controlled base-of-scarp deposits. *Basin Research*, 33(2), 1056–1075. https://doi.org/10.1111/bre.12505

Chiarella, D. & Gioia, D. (2021) A graphic method for depicting basin evolution and changes in the dominant hydrodynamic process from paleocurrent data. *Geosphere*, 17(6), 1861–1868. https://doi.org/10.1130/ges02403.1

Chiarella, D. & Longhitano, S.G. (2012) Distinguishing depositional environments in shallow water mixed, bio-siliciclastic deposits on the base of the degree of heterolithic segregation (Gelasian, southern Italy). *Journal of Sedimentary Research*, 82, 969–990.

Chiarella, D., Longhitano, S.G. & Muto, F. (2012a) Sedimentary features of the Lower Pleistocene mixed siliciclastic-bioclastic tidal deposits of the Catanzaro Strait (Calabrian Arc, south Italy). *Rendiconti Online della Società Geologica Italiana*, 21(PART 2), 919–920.

Chiarella, D., Longhitano, S.G., Sabato, L. & Tropeano, M. (2012b) Sedimentology and hydrodynamics of mixed (siliciclastic–bioclastic) shallow-marine deposits of Acerenza (Pliocene, Southern Apennines, Italy). *Italian Journal of Geosciences*, 131, 136–151.

Chiarella, D., Longhitano, S.G. & Tropeano, M. (2017) Types of mixing and heterogeneities in siliciclastic-carbonate sediments. *Marine and Petroleum Geology*, 88, 617–627. https://doi.org/10.1016/j.marpetgeo.2017.09.010

Chiarella, D., Longhitano, S.G. & Tropeano, M. (2019) Different stacking patterns along an active fold-and-thrust belt—Acerenza Bay, Southern Apennines (Italy). *Geology*, 47(2), 139–142. https://doi.org/10.1130/g45628.1

Ciaranfi, N., Pieri, P. & Ricchetti, G. (1988) Note alla Carta Geologica delle Murge e del Salento (Puglia centro-meridionale). *Memorie della Societa Geologica Italiana*, 41, 449–460.

Clari, P.A., Dela Pierre, F. & Martire, L. (1995) Discontinuities in carbonate successions: identification, interpretation and classification of some Italian examples. *Sedimentary Geology*, 100, 97–121.

Colella, A. (1995) Sedimentation, deformational events and eustacy in the perityrrhenian Amantea Basin: preliminary synthesis. *Giornale di Geologia*, 57, 179–193.

Costello, W.R. & Southard, J.B. (1981) Flume experiments on lower-regime bedforms in coarse sands. *Journal of Sedimentary Petrology*, 51, 849–864.

Coughenour, C.L., Archer, A.W. & Lacovara, K.J. (2009) Tides, tidalites, and secular changes in the Earth–Moon system. *Earth-Science Reviews*, 97, 59–79.

Dalrymple, R.W. (1984) The morphology of internal structure of sandwaves in the Bay of Fundy. *Sedimentology*, 31, 365–382.

Dalrymple, R.W. (2010) Tidal depositional systems. In: James, N.P. & Dalrymple, R.W. (Eds.) *Facies models 4*, Vol. 4. Calgary: Geological Association of Canada, pp. 201–231.

Dalrymple, R.W., Knight, R.J., Zaitlin, B.A. & Middelton, G.V. (1990) Dynamics and facies model of a macrotidal sand-bar complex, Cobequid Bay-Salmon River Estuary (Bay of Fundy). *Sedimentology*, 37, 577–612.

Dalrymple, R.W. & Rhodes, R.N. (1995) Estuarine dunes and barforms, in geomorphology and sedimentology of estuaries. In: Perillo, G.M. (Ed.) *Developments in Sedimentology*. Amsterdam: Elsevier, pp. 359–422.

D'Argenio, B., Ferreri, V. & Amodio, S. (2008) Sequence stratigraphy of Cretaceous carbonate platforms: a cyclostratigraphic approach. In: Amorosi, A., Haq, B.U., Sabato, L. (Eds.) *Advances in application of sequence stratigraphy in Italy*. Geoacta Special Publication 1, 151–171.

D'Argenio, B., Ferreri, V., Raspini, A., Amodio, S. & Buonocunto, F.P. (1999) Cyclostratigraphy of a carbonate platform as a tool for high-precision correlation. *Tectonophysics*, 315, 357–385.

D'Argenio, B., Ferreri, V., Weissert, H., Amodio, S., Buonocunto, F. & Wissler, L. (2004) A multi-disciplinary approach to global correlation and geochronology. The Cretaceous shallow-water carbonates of southern Appennines, Italy. In: D'Argenio, B., Fischer, A.G., Premoli Silva, I., Weissert, H., Ferreri, V. (Eds.) *Cyclostratigraphy, approaches and case histories*. SEPM Special Publication, vol. 81, pp. 103–122.

Davis, R.A., Jr. & Dalrymple, R.W. (2012) *Principles of tidal sedimentology*. Dordrecht: Springer, p. 638.

Devine, P.E. (1991) Transgressive origin of channeled estuarine deposits in the Point Lookout Sandstone, Northwestern New Mexico: a model for Upper Cretaceous, cyclic regressive parasequences of the U.S. western interior. *AAPG Bulletin*, 75, 1039–1063.

Di Stefano, A. & Longhitano, S.G. (2009) Tectonics and sedimentation of the Lower and Middle Pleistocene mixed bioclastic/siliciclastic sedimentary succession of the Ionian Peloritani Mts (NE Sicily, southern Italy): the onset of the Messina Strait opening. *Central European Journal of Geosciences*, 1, 33–62.

Elfenbein, C., Husby, Ø. & Ringrose, P.S. (2005) Geologically-based estimation of kv/kh ratios: an example from the Garn Formation, Tyrihans Field, Mid-Norway. In: Doré, A.G., Vining, B.A. (Eds.) *Petroleum geology: Northwest Europe and Global Perspectives*. Proceedings of the 6th Petroleum Geology Conference Geological Society of London, pp. 537–544.

Eltom, H.A., Saraih, N.A., Esteva, O.G., Kusuma, L., Ahmed, S. & Yassin, M.A. (2020) Three-dimensional modeling and fluid flow simulation for the quantitative description of permeability anisotropy in tidal flat carbonate. *Energies*, 13(21), 5557. https://doi.org/10.3390/en13215557

Enos, P. & Sawatsky, L.H. (1981) Pore networks in Holocene carbonate sediments. *Journal of Sedimentary Petrology*, 51, 961–985.

Esteban, M. & Klappa, C.F. (1983) Subaerial exposure environment. In: P.A. Scholle, D.G. Bebout and C. Moore (Eds.) Carbonate depositional environments. AAPG Memories 33, 1–54.

Feng, J., Cao, J., Hu, K., Peng, X., Chen, Y., Wang, Y. & Wang, M. (2013) Dissolution and its impacts on reservoir formation in moderately to deeply buried strata of mixed siliciclastic-carbonate sediments, north western Qaidam Basin, northwest China. *Marine and Petroleum Geology*, 39, 124–137.

Flügel, E. (2004) *Microfacies of carbonate rock: analysis, interpretation and application*. Berlin: Springer-Verlag, p. 976.

Furre, A.-K., Meneguolo, R., RIngrose, P. & Kassold, S. (2019) Building confidence in CCS: from Sleipner to the Northern light project. *First Break*, 37, 81–87.

Grammer, G., Harris, P. & Eberli, G. (2004) Integration of outcrop and modern analogs in reservoir modeling: overview and examples from the Bahamas, in Integration of outcrop and modern analogs in reservoir modeling. *AAPG Memoir*, 80, 1–22.

Halley, R.B. & Beach, D.K. (1979) Porosity preservation and early freshwater diagenesis of marine carbonate sands. *AAPG Bulletin*, 63, 460.

Halley, R.B. & Schmoker, J.W. (1983) High-porosity Cenozoic carbonate rocks of south Florida: progressive loss of porosity with depth. *AAPG Bulletin*, 67, 191–200.

Hillgärtner, H. (1998) Discontinuity surfaces on a shallow-marine carbonate platform (Berriasian, Valanginian), France and Switzerland. *Journal of Sedimentary Research*, 68, 1093–1108.

Hippolyte, J.C., Angelier, J., Roure, F. & Casero, P. (1994) Piggyback basin development and thrust belt evolution: structural and paleostress analyses of Plio-Quaternary basins in the southern Apennines. *Journal of Structural Geology*, 16, 159–173.

Hossain, S., Hampson, G.J., Jacquemyn, C., Jackson, M.D. & Chiarella, D. (2024) Permeability characterisation of sedimentological facies in the Bunter Sandstone Formation, endurance CO_2 storage site, Offshore UK. *International Journal of Greenhouse Gas Control*, 135, 104140.

Issautier, B., Fillacier, S., Le Gallo, Y., Audigane, P., Chiaberge, C. & Viseur, S. (2013) Modelling of CO_2 injection in fluvial sedimentary heterogeneous reservoirs to assess the impact of geological heterogeneities on CO_2 storage capacity and performance. *Energy Procedia*, 37, 5181–5190. https://doi.org/10.1016/j.egypro.2013.06.434

Jackson, M.D., Yoshida, S., Johnson, H.D., Muggeridge, A.H., Næss, A. & Ringrose, P.S. (1999) Three-dimensional reconstruction, flow simulation, and upscaling of complex bedform-scale sedimentary structures within tidal sandstone reservoirs. In: Hentz, T.F. (Ed.) *Advanced reservoir characterization for the twenty-first century*. SEPM Gulf Coast Section 19th Annual Research Conference Proceedings Houston, pp. 169–178.

Jackson, M.D., Yoshida, S., Muggeridge, A.H. & Johnson, H.D. (2005) Three-dimensional reservoir characterisation and flow simulation of heterolithic tidal sandstones. *American Association of Petroleum Geologists Bulletin*, 89, 507–528.

Jackson, M.D., Hampson, G.J. & Sech, R.P. (2009) Three-dimensional modeling of a shoreface-shelf parasequence reservoir analog: part 2. Geologic controls on fluid flow and hydrocarbon recovery. *American Association of Petroleum Geologists Bulletin*, 93, 1183–1208.

Jackson, M.D., Hampson, G.J., Saunders, J.H., El-Sheikh, A., Graham, G.H. & Massart, B.Y.G. (2013) Surface-based reservoir modelling for flow simulation. *Geological Society, London, Special Publications*, 387(1), 271–292. https://doi.org/10.1144/sp387.2

Jackson, W.A., Hampson, G.J., Jacquemyn, C., Jackson, M.D., Petrovskyy, D., Geiger, S., Machado Silva, J.D., Judice, S., Rahman, F. & Costa Sousa, M. (2022) A screening assessment of the impact of sedimentological heterogeneity on CO_2 migration and stratigraphic-baffling potential: Johansen and Cook formations, Northern Lights project, offshore Norway. *International Journal of Greenhouse Gas Control*, 120, 103762.

Jacquemyn, C.E.M.M., Pataki, M.E.H., Hampson, G.J., Jackson, M.D., Petrovskyy, D., Geiger, S., Silva, J.D.M., Judice, S., Rahman, F., Silva, C.C.M.M. & Costa Sousa, M. (2021) Sketch-based interface and modelling of stratigraphy and structure in 3D. *Journal of the Geological Society of London*, 178, 2020–2187.

James, N.P., Seibel, M.J., Dalrymple, R.W., Besson, D. & Parize, O. (2014) Warm-temperate, marine, carbonate sedimentation in an Early Miocene, tide-influenced, incised valley; Provence, south-east France. *Sedimentology*, 61, 497–534. https://doi.org/10.1111/sed.12063

Khan, M.A., Khan, T., Ali, A., Bello, A.M. & Radwan, A.E. (2023) Role of depositional and diagenetic controls on reservoir quality of complex heterogenous tidal sandstone reservoirs: an example from the Lower Goru formation, Middle Indus Basin, Southwest Pakistan. *Marine and Petroleum Geology*, 154, 106337. https://doi.org/10.1016/j.marpetgeo.2023.106337

Kupecz, J.A., Gluyas, J. & Bloch, S. (1997) Reservoir quality prediction in sandstones and carbonates. *AAPG Memoir*, 69, 316.

Kvale, E.P. (2003) Tides and tidal rhythmites. In: Middleton, G.V. (Ed.) *Encyclopedia of sediments and sedimentary rocks*. Dordrecht: Kluwer Academic, pp. 741–744.

Leva López, J., Rossi, V.M., Olariu, C. & Steel, R.J. (2016) Architecture and recognition criteria of ancient shelf ridges; an example from Campanian Almond Formation in Hanna Basin, USA. *Sedimentology*, 63(6), 1651–1676. https://doi.org/10.1111/sed.12279

Li, J., Geiger, S., Costa Gomes, J., Petrovsky, D., Jacquemyn, C., Hampson, G.J., Jackson, M.D., Machado Silva, J., Judice, S., Rahman, F. & Costa Sousa, M. (2022) Fast assessment of the impact of multi-scale geological heterogeneities on flow behaviour in complex carbonate reservoirs. EAGE 83rd Conference & Exhibition, Madrid, Spain.

Longhitano, S.G. & Nemec, W. (2005) Statistical analysis of bed-thickness variation in a Tortonian succession of biocalcarenitic tidal dunes, Amantea Basin, Calabria, southern Italy. *Sedimentary Geology*, 179, 195–224.

Longhitano, S.G. (2011) The record of tidal cycles in mixed silici-bioclastic deposits: examples from small Plio-Pleistocene peripheral basins of the microtidal central Mediterranean Sea. *Sedimentology*, 58, 691–719.

Longhitano, S.G., Mellere, D., Steel, R.J. & Ainsworth, R.B. (2012a) Tidal depositional systems in the rock record: a review and new insights. In: Longhitano, S.G., Mellere, D., Ainsworth, B. (Eds.) Modern and ancient tidal depositional systems: perspectives, models and signatures. Sedimentary Geology, 279, 2–22.

Longhitano, S.G., Chiarella, D., Di Stefano, A., Messina, C., Sabato, L. & Tropeano, M. (2012b) Tidal signatures in Neogene to Quaternary mixed deposits of southern Italy straits and bays. In: Longhitano, S.G., Mellere, D., Ainsworth, B. (Eds.) Modern and ancient tidal depositional systems: perspectives, models and signatures. Sedimentary Geology 279, 74–96.

Longhitano, S.G., Chiarella, D. & Spalluto, L. (2012c) Tidal facies in siliciclastic, carbonate and mixed microtidal ancient systems of southern Italy. Tidalites 2012, 8th International Conference on tidal environments, Caen, France.

Longhitano, S.G., Zecchin, M., Chiarella, D., Prosser, G. & Muto, F. (2012d) Tectonics and Sedimentation in Neogene-to-Quaternary

Sedimentary Basins of Central Calabria (South Italy). A 4-days-long Field Course for Petroleum Geologists and Geophysicists, 62 p.

Longhitano, S.G. (2013) A facies-based depositional model for ancient and modern, tectonically-confined tidal straits. *Terra Nova*, 25, 446–452.

Longhitano, S.G. & Chiarella, D. (2020) Tidal straits: basic criteria for recognizing ancient systems from the rock record. *Regional Geology and Tectonics: Principles of Geologic Analysis*, 365–415. https://doi.org/10.1016/b978-0-444-64134-2.00014-6

Longhitano, S.G., Chiarella, D. & Muto, F. (2014) Three-dimensional to two-dimensional cross-strata transition in the lower Pleistocene Catanzaro tidal strait transgressive succession (southern Italy). *Sedimentology*, 61, 2136–2171.

Longhitano, S.G., Tropeano, M., Chiarella, D., Festa, V., Mateu-Vicens, G., Pomar, L., Sabato, L. & Spalluto, L. (2021) The sedimentary response of mixed lithoclastic-bioclastic Lower- Pleistocene shallow-marine systems to tides and waves in the south Apennine foredeep (Basilicata, southern Italy) Tidalites Field Trips Special Volume – Tidalites, Matera, Field Trip T3. *Geological Field Trips*, 13(2.3), 1–54. https://doi.org/10.3301/gft.2021.07

Major, R.P. & Holtz, M.H. (1997) Predicting reservoir quality at the development scale: methods for quantifying remaining hydrocarbon resource in diagenetically-complex carbonate reservoirs. In: Kupecz, J.A., Gluyas, J., Bloch, S. (Eds.) Reservoir quality predictions in sandstone and carbonates. AAPG Memoir, vol. 69, pp. 231–248.

Mansurbeg, H., Caja, M.A., Marfil, R., Morad, S., Remacha, E., Garcia, D., Martín-Crespo, T., El-Ghali, M.A.K. & Nystuen, J.P. (2009) Diagenetic evolution and porosity destruction of turbiditic hybrid arenites and siliciclastic sandstones of Foreland Basins: evidence from the Eocene Hecho Group, Pyrenees, Spain. *Journal of Sedimentary Research*, 79, 711–735.

Martinius, A.W., Kaas, I., Næss, A., Helgesen, G., Kjærefjord, J.M. & Leith, D.A. (2001) Sedimentology of the heterolithic and tide-dominated Tilje Formation (Early Jurassic, Halten Terrace, offshore mid-Norway). In: Martinsen, O.J., Dreyer, T. (Eds.) *Sedimentary environments offshore Norway—Palaeozoic to recent*. Norwegian Petroleum Society (NPF) Special Publication, vol. 10, pp. 103–144.

Martinius, A.W., Ringrose, P.S., Brostrøm, C., Elfenbein, C., Næss, A. & Ringås, J.E. (2005) Reservoir challenges of heterolithic tidal sandstone reservoirs in the Halten Terrace, mid-Norway. *Petroleum Geoscience*, 11, 3–16.

Massart, B.Y.G., Jackson, M.D., Hampson, G.J., Legler, B., Johnson, H.D., Jackson, C.A.-L., Breheret, A.M., Daboer, J., Onokwai, N., Talabi, O., Ravnas, R. & Sarginson, M. (2012) Three-dimensional surface-based modeling and flow simulation of heterolithic tidal sandstone reservoirs. American Association of Petroleum Geologists, Annual Convention and Exhibition, Long Beach, CA, April 22–25.

Massart, B.Y.G., Jackson, M.D., Hampson, G.J., Johnson, H.D., Legler, B. & Jackson, C.A.-L. (2016a) Effective flow properties of heterolithic, cross-bedded tidal sandstones: Part 1. Surface-based modeling. *AAPG Bulletin*, 100(5), 697–721. https://doi.org/10.1306/02011614221

Massart, B.Y.G., Jackson, M.D., Hampson, G.J. & Johnson, H.D. (2016b) Effective flow properties of heterolithic, cross-bedded tidal sandstones: Part 2. Flow simulation. *AAPG Bulletin*, 100(5), 723–742. https://doi.org/10.1306/02011614222

Mazzullo, S.J. (2004) Overview of porosity evolution in carbonate reservoirs. *Kansas Geological Survey*, 79, 22–28.

Melim, L.A., Westphal, H., Swart, P.K., Eberli, G.P. & Munnecke, A. (2002) Questioning carbonate diagenetic paradigms: evidence from the Neogene of The Bahamas. *Marine Geology*, 185, 27–53.

Meneguolo, R., Sundal, A., Martinius, A.W., Veselovsky, Z., Cullum, A. & Milovanova, E. (2022) Impact of the lower Jurassic Dunlin Group depositional elements on the Aurora CO_2 storage site, EL001, northern North Sea, Norway. *International Journal of Greenhouse Gas Control*, 119, 103723.

Meyer, R. & Krause, F.F. (2001) A comparison of plug- and probe-derived permeabilities in cross-bedded sandstones of the Virgelle Member, Alberta, Canada: The influence of flow directions on probe permeametry. *AAPG Bulletin*, 85(477), 489.

Meyer, R. (2002) Anisotropy of sandstone permeability. CREWES Research Report 14, 12 p.

Mercier, D., Barrier, P., Beaudoin, B., Didier, S., Montenat, J.L. & Salinas Zuniga, E. (1987) Les facteurs hydrodynamiques dans la sédimentasion plio-quaternaire du Détroit de Messine. Le Détroit de Messine (Italie). Evolution tectono-sedimentaire récente (Pliocéne et Quaternaire) et environment actuel. Doc. Trav. IGAL (Paris), vol. 11, pp. 171–183.

Messina, C. & Nemec, W. (2006) *Sedimentological and statistical analysis of the Garn Formation in the Kristin field*. Trondheim: Report to Statoil Research Centre, p. 82.

Messina, C., Nemec, W., Martinius, A.W. & Elfenbein, C. (2014) The Garn Formation (Bajocian-Bathonian) in the Kristin Field, Halten Terrace: its origin, facies architecture and primary heterogeneity model. IAS Special Publication. In: Martinius, A.W., Howell, J., Olsen, T., Ravnås, R., Steel, R.J., Wonham, J. (Eds.) *From depositional systems to sedimentary successions on the Norwegian Continental Shelf*. International Association of Sedimentologists Special Publication vol. 46 (in press).

Mindszenty, A., D'Argenio, B. & Aiello, G. (1995) Lithospheric bulges recorded by regional unconformities. The case of Mesozoic-Tertiary Apulia. *Tectonophysics*, 252, 137–161.

Mishra, A., Kurtev, K.D. & Haese, R.R. (2020) Composite rock types as part of a workflow for the integration of mm-to cm-scale lithological heterogeneity in static reservoir models. *Marine and Petroleum Geology*, 114, 104240. https://doi.org/10.1016/j.marpetgeo.2020.104240

Moore, C.H. (1989) *Carbonate diagenesis and porosity: developments in Sedimentology, vol. 46*. New York: Elsevier, p. 338.

Morad, S., Ketzer, J.M. & De Ros, L.F. (2013) Linking diagenesis to sequence stratigraphy: an integrated tool for understanding and predicting reservoir quality distribution. In: Morad, S., Ketzer, J.M. & De Ros, L.F. (Eds.) *Linking diagenesis to sequence stratigraphy*. Hoboken: Wiley-Blackwell, https://doi.org/10.1002/9781118485347.ch1

Newell, A.J., Pourmalek, A., Butcher, A.S. & Shariatipour, S.M. (2019) The importance of lithofacies control on fluid migration in heterogeneous aeolian formations for geological CO_2 storage: lessons from observational evidence and modelling of bleached palaeoreservoirs at Salt Wash Graben, Utah. *International Journal of Greenhouse Gas Control*, 91, 102841. https://doi.org/10.1016/j.ijggc.2019.102841

Nordahl, K., Ringrose, P.S. & Wen, R. (2005) Petrophysical characterization of a heterolithic tidal reservoir interval using a process-based modelling tool. *Petroleum Geoscience*, 11, 17–28.

Nordahl, K. & Ringrose, P.S. (2008) Identifying the representative elementary volume for permeability in heterolithic deposits using numerical rock models. *Mathematical Geoscience*, 70, 753–771.

Olariu, C., Steel, R.J., Dalrymple, R.W. & Gingras, M.K. (2012) Tidal dunes versus tidal bars: The sedimentological and architectural characteristics of compound dunes in a tidal seaway, the lower Baronia Sandstone (Lower Eocene), Ager Basin, Spain. In: S.G. Longhitano, D. Mellere, and B. Ainsworth (Eds.) Modern and ancient tidal depositional systems: perspectives, models and signatures. Sedimentary Geology, 279, 134–155.

Olierook, H.K.H., Delle Piane, C., Timms, N.E., Esteban, L., Rezaee, R., Mory, A.J. & Hancock, L. (2014) Facies-based rock properties characterization for CO_2 sequestration: GSWA Harvey 1 well, Western Australia. *Marine and Petroleum Geology*, 50, 83–102. https://doi.org/10.1016/j.marpetgeo.2013.11.002

Payton, R.L., Chiarella, D. & Kingdon, A. (2021) Pore-scale assessment of subsurface carbon storage potential: implications for the UK Geoenergy Observatories project. *Petroleum Geoscience*, 27, 020092.

Payton, R.L., Chiarella, D. & Kingdon, A. (2022a) The upper percolation threshold and porosity–permeability relationship in sandstone reservoirs using digital image analysis. *Scientific Reports*, 12, 11311. https://doi.org/10.1038/s41598-022-15651-3

Payton, R.L., Chiarella, D. & Kingdon, A. (2022b) The influence of grain shape and size on the relationship between porosity and permeability in sandstone: a digital approach. *Scientific Reports*, 12, 7531. doi:10.1038/s41598-022-11365-8

Paxton, S.T., Szabo, J.O., Ajdukiewicz, J.M. & Klimentidis, R.E. (2002) Construction of an inter-granular volume compaction curve for evaluating and predicting compaction and porosity loss in rigid-grain sandstone reservoirs. *AAPG Bulletin*, 86(12), 2047–2067.

Pescatore, T., Renda, P., Schiattarella, M. & Tramutoli, M. (1999) Stratigraphic and structural relationships between Meso-Cenozoic Lagonegro basin and coeval carbonate platforms in southern Apennines, Italy. *Tectonophysics*, 315, 269–286.

Pickup, G.E. & Hern, C.Y. (2002) The development of appropriate upscaling procedures. *Transport in Porous Media*, 46, 119–138.

Pickup, G.E., Ringrose, P.S., Jensen, J.L. & Sorbie, K.S. (1994) Permeability tensors for sedimentary structures. *Mathematical Geology*, 26(2), 227–250.

Pieri, P., Sabato, L., Loiacono, F. & Marino, M. (1994) Il bacino di piggy back di Sant'Arcangelo: evoluzione tettonico-sedimentaria. *Bollettino della Societa Geologica Italiana*, 113, 465–481.

Posamentier, H.W. (2002) Ancient shelf ridges—a potentially significant component of the transgressive systems tract: case study from offshore northwest Java. *AAPG Bulletin*, 86, 75–106.

Pourmalek, A., Newell, A.J., Shariatipour, S.M., Butcher, A.S., Milodowski, A.E., Bagheri, M. & Wood, A.M. (2021a) Deformation bands in high-porosity sandstones: do they help or hinder CO_2 migration and storage in geological formations? *International Journal of Greenhouse Gas Control*, 107, 103292. https://doi.org/10.1016/j.ijggc.2021.103292

Pourmalek, A., Newell, A.J., Shariatipour, S.M. & Wood, A.M. (2021b) The impact of heterogeneous mixed siliciclastic–carbonate systems on CO_2 geological storage. *Petroleum Geoscience*, 28(1), petgeo2020-086. https://doi.org/10.1144/petgeo2020-086

Pratt, B.R. (2010) Peritidal Carbonates. In: James, N.P. & Dalrymple, R.W. (Eds.) *Facies Models 4. Geological Association of Canada*. Newfoundland: St. John's, pp. 401–420.

Pyrcz, M.J., Catuneanu, O. & Deutsch, C.V. (2005) Stochastic surface-based modeling of turbidite lobes. *AAPG Bulletin*, 89, 177–191.

Quin, J.G., Zweigel, P., Eldholm, E., Hansen, O.R., Christoffersen, K.R. & Zaostrovski, A. (2010) Sedimentology and unexpected pressure decline: the HP/HT Kristin Field. In: Vining, B.A., Pickering, S.C. (Eds.) *Petroleum geology: from mature basins to new frontiers*. Petroleum Geology Conference Series vol. 7, Geological Society of London, pp. 419–429.

Reineck, H.E. & Wunderlich, F. (1968) Classification and origin of flaser and lenticular bedding. *Sedimentology*, 11, 99–104.

Reineck, H.E. & Singh, I.B. (1980) *Depositional sedimentary environments*. Berlin: Springer-Verlag, p. 551.

Ricchetti, G. (1975) Nuovi dati stratigrafici sul Cretaceo delle Murge emersi da indagini nel sottosuolo. *Italian Journal of Geosciences*, 94, 1083–1108.

Ricchetti, G., Ciaranfi, N., Luperto Sinni, E., Mongelli, F. & Pieri, P. (1988) Geodinamica ed evoluzione sedimentaria e tettonica dell'Avampaese apulo. *Memorie della Societa Geologica Italiana*, 41, 57–82.

Ringrose, P.S. & Meckel, T.A. (2019) Maturing global CO_2 storage resources on offshore continental margins to achieve 2DS emissions reductions. *Scientific Reports*, 9, 1–10.

Ringrose, P., Nordahl, K. & Wen, R. (2005) Vertical permeability estimation in heterolithic tidal deltaic sandstones. *Petroleum Geoscience*, 11, 29–36.

Sattler, U., Immhenauser, A., Hillgärtner, H. & Esteban, M. (2005) Characterization, lateral variability and lateral extent of discontinuity surfaces on a carbonate platform (Barremian to Lower Aptian, Oman). *Sedimentology*, 52, 339–361.

Sech, R.P., Jackson, M.D. & Hampson, G.J. (2009) Three-dimensional modeling of a shoreface-shelf parasequence reservoir analog: part 1. Surface-based modeling to capture high-resolution facies architecture. *American Association of Petroleum Geologists Bulletin*, 93, 1155–1181.

Scholle, P.A. & Halley, R.B. (1985) Burial diagenesis: out of sight, out of mind! In: Schneidermann, N., Harris, P.M. (Eds.) Carbonate cements. SEPM Special Publication, vol. 36, pp. 309–334.

Scholle, P.A. & Umer-Scholle, D.S. (2003) Color guide to the petrography of carbonate rocks: grains, textures, porosity, diagenesis. *AAPG Memoir*, 77, 474.

Selli, R. (1962) Il Paleogene nel quadro della geologia dell'Italia meridionale. *Memorie della Societa Geologica Italiana*, 3, 737–789.

Shinn, E.A. (1983) Tidal flat environment. In: Scholle, P.A., Bebout, D.G. Moore, C. (Eds.) Carbonate depositional environments. AAPG Memories, vol. 33, pp. 171–210.

Slatt, R.M. (2006) Stratigraphic reservoir characterization for petroleum geologists, geophysicists and engineers. In: *Handbook of petroleum exploration and production*, Vol. 6. Elsevier.

Southard, J.B. & Boguchwal, L.A. (1990) Bed configurations in steady unidirectional water flow part 2. Synthesis of flume data. *Journal of Sedimentary Petrology*, 60, 658–679.

Spalluto, L., Pieri, P. & Ricchetti, G. (2005) Le facies carbonatiche di piattaforma interna del Promontorio del Gargano: implicazioni paleoambientali e correlazioni con la coeva successione delle Murge (Italia meridionale, Puglia). *Bollettino della Societa Geologica Italiana*, 124, 675–690.

Spalluto, L., Moretti, M., Festa, V. & Tropeano, M. (2007) Seismically-induced slumps in lower-Maastrichtian peritidal carbonates of the Apulian Platform (Southern Italy): towards a methodology for determining the trigger agent for soft-sediment deformation. *Sedimentary Geology*, 196, 81–98.

Spalluto, L. (2008) Sedimentology and high-resolution sequence stratigraphy of a lower Cretaceous shallow-water carbonate succession from the western Gargano Promontory (Apulia, southern Italy). In: Amorosi, A., Haq, B.U., Sabato, L. (Eds.) *Advances in application of sequence stratigraphy in Italy*. Geoacta Special Publication 1, 173–192.

Spalluto, L., Caffau, M. & De Giorgio, G. (2008) The upper Albian-lower Cenomanian inner shelf carbonate succession of the Calcare di Bari Fm. from the Murge area (Apulia, southern Italy). *Rendiconti Online della Società Geologica Italiana*, 2, 181–186.

Spalluto, L. (2012) Facies evolution and sequence chronostratigraphy of a "mid"-Cretaceous shallow-water carbonate succession of the Apulia Carbonate Platform from the northern Murge area (Apulia, southern Italy). *Facies*, 58, 17–36.

Strasser, A. & Davaud, E. (1983) Black pebbles of the Purbeckian (Swiss and French Jura): lithology, geochemistry and origin. *Eclogae Geologicae Helveticae*, 76, 551–580.

Strasser, A. (1991) Lagoonal-peritidal sequences in carbonate environments: autocyclic and allocyclic processes. In: *Cycles and event in stratigraphy*. Berlin: Springer-Verlag, pp. 710–733.

Strasser, A., Pittet, B., Hillgärtner, H. & Pasquier, J.B. (1999) Depositional sequences in shallow carbonate-dominated sedimentary systems: concepts for a high-resolution analysis. *Sedimentary Geology*, 128, 201–221.

Strasser, A., Hillgartner, H., Hug, W. & Pittet, B. (2000) Third-order depositional sequences reflecting Milankovitch cyclicity. *Terra Nova*, 12, 303–311.

Strasser, A. (2018) Cyclostratigraphy of shallow-marine carbonates—limitations and opportunities. *Stratigraphy and Timescales*, 3, 151–187.

Suarez-Gonzalez, P., Quijada, I.E., Benito, M.I., Mas, R., Merinero, R. & Riding, R. (2014) Origin and significance of lamination in Lower Cretaceous stromatolites and proposal for a quantitative approach. *Sedimentary Geology*, 300, 11–27.

Sun, X., Cao, Y., Liu, K., Alcalde, J., Cabello, P., Travé, A., Cruset, D. & Gomez-Rivas, E. (2023) Effects of fluvial sedimentary heterogeneity on CO_2 geological storage: integrating storage capacity, injectivity, distribution and CO_2 phases. *Journal of Hydrology*, 617, 128936. https://doi.org/10.1016/j.jhydrol.2022.128936

Sundal, A., Hellevang, H., Miri, R., Dypvik, H., Nystuen, J.P. & Aagaard, P. (2014) variations in mineralisation potential for CO_2 related to sedimentary facies and burial depth—a comparative study from the North Sea. *Energy Procedia*, 63, 5063–5070.

Sundal, A., Nystuen, J.P., Rørvik, K., Dypvik, H. & Aagaard, P. (2016) The lower Jurassic Johansen formation, northern North Sea—depositional model and reservoir characterization for CO_2 storage. *Marine and Petroleum Geology*, 77, 1376–1401.

Trevisan, L., Krishnamurthy, P.G. & Meckel, T.A. (2017a) Impact of 3D capillary heterogeneity and bedform architecture at the sub-meter scale on CO_2 saturation for buoyant flow in clastic aquifers. *International Journal of Greenhouse Gas Control*, 56, 237–249.

Trevisan, L., Pini, R., Cihan, A., Birkholzer, J.T., Zhou, Q., González-Nicolás, A. & Illangasekare, T.H. (2017b) Imaging and quantification of spreading and trapping of carbon dioxide in saline aquifers using meter-scale laboratory experiments. *Water Resources Research*, 53(1), 485–502. https://doi.org/10.1002/2016wr019749

Tortorici, L. (1982) Lineamenti geologico-strutturali dell'Arco Calabro Peloritano. *Società Italianas Mineralogia e Petrografia*, 38, 927–940.

Vail, P.R., Audemard, F., Bowman, S.A., Eisner, P.N. & Perez Cruz, C. (1991) The stratigraphic signatures of tectonics, eustasy and sedimentology—an overview. In: Einsele, G., Ricken, W. & Seilacher, A. (Eds.) *Cycles and events in stratigraphy*. Berlin: Springer-Verlag, pp. 617–662.

Valduga, A. (1965) Contributo alla conoscenza geologica delle Murge baresi. *Studi geologici e geomorfologici sulla regione Pugliese*, 1, 1–14.

Vezzani, L. (1967) I depositi plio-pleistocenici del litorale ionico della Lucania. *Atti Accademia Gioenia Scienze Naturali*, 18, 159–180.

Weber, K.J. (1986) How heterogeneity affects oil recovery. In: Lake, L.W. & Carroll, H.B., Jr. (Eds.) *Reservoir characterization*. Orlando: Academic Press, pp. 487–544.

Weber, K.J. & Van Geuns, L.C. (1990) Framework for constructing clastic reservoir simulation models. *Journal of Petroleum Technology*, 42(1248–1253), 1296–1297.

Wen, R.-J., Martinius, A.W., Næss, A. & Ringrose, P.S. (1998) Three-dimensional simulation of small-scale heterogeneity in tidal deposits—a process-based stochastic method. In: A. Buccianti, G. Nardi and A. Potenza (Eds.) Proceedings 4th Annual Conference of the International Association of Mathematical Geology, pp. 129–134. De Frede, Naples.

White, C.D. & Barton, M.D. (1999) Translating outcrop data to flow models, with applications to the Ferron sandstone. *Society of Petroleum Engineers Reservoir Evaluation and Engineering*, 2, 341–350.

White, C.D., Willis, B.J., Dutton, S.P., Bhattacharya, J.P., Narayanan, K., Eberli, G.P., Harris, P.M. & Grammer, G.M. (2004) Sedimentology, statistics, and flow behavior for a tide-influenced deltaic sandstone, frontier formation, Wyoming, United States. In: Integration of Outcrop and Modern Analogs in Reservoir Modeling, vol. 80. American Association of Petroleum Geologists Memoir, pp. 291–323.

Williams, G.E. (1991) Upper Proterozoic tidal rhythmites, South Australia: sedimentary features, deposition, and implications for the earth's palaeorotation. In: A. Smith, G.E. Reinson, B.A. Zaitlin, and R.A. Rahmani (Eds.) Clastic tidal sedimentology. Canadian Society of Petroleum Geology Memories 16, 161–177.

Wonham, J.P., Cyrot, M., Nguyen, T., Louhouamou, J. & Ruau, O. (2010) Integrated approach to geomodelling and dynamic simulation in a complex mixed siliciclastic–carbonate reservoir, N'Kossa field, Offshore Congo. In: Jolley, S. J., Fisher, Q. J., Ainsworth, R. B., Vrolijk, P. J., Delisle, S. (Eds.) *Reservoir compartmentalization*. Geological Society of London Special Publications, vol. 347, pp. 133–164.

Zhang, X., Pyrcz, M.J. & Deutch, C.V. (2009) Stochastic surface modeling of deepwater depositional systems for improved reservoir models. *Journal of Petroleum Science and Engineering*, 68, 118–134.

How to cite this article: Chiarella, D., Longhitano, S.G., Spalluto, L. & Martinius, A.W. (2024) Hierarchies of stratigraphic discontinuity surfaces in siliciclastic, carbonate and mixed siliciclastic-bioclastic tidalites: Implications for fluid migration in reservoir quality assessment. *The Depositional Record*, 00, 1–30. Available from: https://doi.org/10.1002/dep2.307